NASA Contractor Report 189565
ICASE Report No. 91–82

ICASE

A NEAR-WALL TWO-EQUATION MODEL FOR COMPRESSIBLE TURBULENT FLOWS

H. S. Zhang
R. M. C. So
C. G. Speziale
Y. G. Lai

Contract No. NAS1–18605
November 1991

Institute for Computer Applications in Science and Engineering
NASA Langley Research Center
Hampton, Virginia 23665–5225

Operated by the Universities Space Research Association

National Aeronautics and
Space Administration

Langley Research Center
Hampton, Virginia 23665-5225

A NEAR-WALL TWO-EQUATION MODEL FOR COMPRESSIBLE TURBULENT FLOWS

H. S. Zhang and R. M. C. So
Arizona State University
Tempe, AZ 85287

C. G. Speziale*
ICASE, NASA Langley Research Center
Hampton, VA 23665

Y. G. Lai
CFD Research Corporation
Huntsville, AL 35802

ABSTRACT

A near-wall two-equation turbulence model of the $K-\varepsilon$ type is developed for the description of high-speed compressible flows. The Favre-averaged equations of motion are solved in conjunction with modeled transport equations for the turbulent kinetic energy and solenoidal dissipation wherein a variable density extension of the asymptotically consistent near-wall model of So and co-workers is supplemented with new dilatational models. The resulting compressible two-equation model is tested in the supersonic flat plate boundary layer – with an adiabatic wall and with wall cooling – for Mach numbers as large as 10. Direct comparisons of the predictions of the new model with raw experimental data and with results from the $K-\omega$ model indicate that it performs well for a wide range of Mach numbers. The surprising finding is that the Morkovin hypothesis, where turbulent dilatational terms are neglected, works well at high Mach numbers provided that the near wall model is asymptotically consistent. Instances where the model predictions deviate from the experiments appear to be attributable to the assumption of constant turbulent Prandtl number – a deficiency that will be addressed in a future paper.

*This research was supported by the National Aeronautics and Space Administration under NASA Contract No. NAS1-18605 while the author was in residence at the Institute for Computer Applications in Science and Engineering (ICASE), NASA Langley Research Center, Hampton, VA 23665.

1. INTRODUCTION

The direct numerical simulation of compressible turbulent flows – at high Reynolds numbers with all scales resolved – will not be possible for the foreseeable future, if ever at all. Turbulence modeling will continue to play a crucial role in the computation of high-speed aerodynamic flows associated with the design of advanced aircraft. In these applications, near-wall turbulence modeling is extremely important for the accurate prediction of wall transport properties, such as the skin friction and heat transfer coefficients, which are pivotal for design. Despite its technological importance, progress in near-wall turbulence modeling has been slow. Many of the commonly used near-wall models – which typically contain a variety of ad hoc wall damping functions – are not asymptotically consistent and yield poor predictions even in simple incompressible boundary layers (see Patel, Rodi and Scheuerer[1], Myong and Kasagi[2] and Speziale, Abid and Anderson[3]). These deficiencies can be fatal when turbulence models are applied to separated flows, or other complex boundary layers, that require the governing equations to be integrated directly to the wall.

High-speed compressible flows present a whole range of new problems to near-wall turbulence modeling. Shock/boundary layer interactions with turbulence amplification and flow separation represent but two examples. Two-dimensional equilibrium turbulent boundary layers for supersonic flows are less of a problem provided that the external Mach number M_∞ is not too large. For these flows it is generally believed that Morkovin's hypothesis[4] – commonly interpreted to mean that the turbulence statistics are only altered by compressibility effects through changes in the mean density – is valid for at least the range $0 \leq M_\infty \leq 5$. This hypothesis allows for the use of variable density extensions of existing incompressible turbulence models for which dilatational effects are neglected. However, even the ability of these models to reliably predict mean velocity profiles in two-dimensional equilibrium boundary layers for Mach numbers $M_\infty \geq 5$ has been recently called into question (see Bradshaw, Launder and Lumley[5] and Huang, Bradshaw and Coakley[6]). Of course, for non-equilibrium compressible flows involving shocks – or extremely high Mach numbers in or near the hypersonic flow regime – issues related to near wall turbulence modeling are even more unsettled (c.f. Bushnell[7]).

In this paper, a new near-wall two-equation turbulence model of the $K - \varepsilon$ type is developed for high-speed compressible flows. Two features distinguish this model from earlier work: (a) a variable density extension of the asymptotically consistent near-wall model of So et al.[8] for incompressible flows is used, and (b) high-Reynolds number models for the dilatational terms are implemented as developed recently by Sarkar et al.[9,10] and Coleman and Mansour[11] based on an analysis of homogeneous turbulence. The resulting compressible model is tested in supersonic flat plate boundary layers at zero pressure gradient – both

with an adiabatic wall and with wall cooling – for external Mach numbers in the range $0 \leq M_\infty \leq 10$. Comparisons are made with experimental data, and with the predictions of the $K-\omega$ model of Wilcox[12], in an attempt to address the following questions:

(a) Can incompressible two-equation models be extended to supersonic boundary layers with a minimum of compressible corrections that are systematically determined?

(b) Will these models perform well at high Mach numbers?

(c) Where will the models break down, and what deficiencies give rise to it?

These issues will be addressed in detail in the sections to follow and recommendations will be made for future research.

2. THE TWO-EQUATION TURBULENCE MODEL

We consider the supersonic turbulent flow of an ideal gas with bulk viscosity and body forces neglected. The equations of motion are given by:

Mass

$$\frac{\partial \rho}{\partial t} + (\rho u_i)_{,i} = 0 \tag{1}$$

Momentum

$$\frac{\partial}{\partial t}(\rho u_i) + (\rho u_i u_j)_{,j} = -p_{,i} - \frac{2}{3}(\mu u_{j,j})_{,i} + [\mu(u_{i,j} + u_{j,i})]_{,j} \tag{2}$$

Energy

$$\frac{\partial}{\partial t}(\rho C_p T) + (\rho u_i C_p T)_{,i} = \frac{\partial p}{\partial t} + u_i p_{,i} + \sigma_{ij} u_{i,j} + (kT_{,i})_{,i} \tag{3}$$

where

$$p = \rho R T \tag{4}$$

$$\sigma_{ij} = -\frac{2}{3}\mu u_{k,k}\delta_{ij} + \mu(u_{i,j} + u_{j,i}) \tag{5}$$

are, respectively, the thermodynamic pressure and viscous stress tensor given that ρ is the density, u_i is the velocity, T is the temperature, R is the ideal gas constant, μ is the dynamic viscosity, k is the thermal conductivity, and C_p is the specific heat at constant pressure. Here, the Einstein summation convention applies to repeated indices and $(\cdot)_{,i}$ denotes a gradient with respect to the spatial coordinate x_i.

Any flow variable $\mathcal{F}$ can be decomposed into mean and fluctuating parts in two ways:

$$\mathcal{F} = \overline{\mathcal{F}} + \mathcal{F}', \quad \mathcal{F} = \tilde{\mathcal{F}} + \mathcal{F}'' \tag{6}$$

where $\overline{\mathcal{F}}$ represents the traditional ensemble average whereas $\tilde{\mathcal{F}}$ represents a Favre average defined by

$$\tilde{\mathcal{F}} = \frac{\overline{\rho \mathcal{F}}}{\overline{\rho}}. \tag{7}$$

The mean equations of motion for compressible turbulence take the form:

$$\frac{\partial \overline{\rho}}{\partial t} + (\overline{\rho}\tilde{u}_i)_{,i} = 0 \tag{8}$$

$$\frac{\partial}{\partial t}(\overline{\rho}\tilde{u}_i) + (\overline{\rho}\tilde{u}_i\tilde{u}_j)_{,j} = -\overline{p}_{,i} - \frac{2}{3}(\overline{\mu}\tilde{u}_{j,j})_{,i} + [\overline{\mu}(\tilde{u}_{i,j} + \tilde{u}_{j,i})]_{,j} - (\overline{\rho}\tau_{ij})_{,j} \tag{9}$$

$$\begin{aligned} \frac{\partial}{\partial t}(\overline{\rho}\overline{C}_p\tilde{T}) + (\overline{\rho}\tilde{u}_i\overline{C}_p\tilde{T})_{,i} \;=\; & \frac{\partial \overline{p}}{\partial t} + \tilde{u}_i\overline{p}_{,i} + \overline{u_i''}\overline{p}_{,i} + \overline{u_i' p_{,i}'} + \overline{\sigma}_{ij}\tilde{u}_{i,j} \\ & + \overline{\sigma}_{ij}\overline{u_{i,j}''} + \overline{\rho}\varepsilon - (\overline{\rho}\overline{C}_p Q_i)_{,i} + (\overline{k}\tilde{T}_{,i})_{,i} \end{aligned} \tag{10}$$

where

$$\tau_{ij} = \widetilde{u_i'' u_j''} \tag{11}$$

$$Q_i = \widetilde{u_i'' T''} \tag{12}$$

$$\overline{\sigma}_{ij} = -\frac{2}{3}\overline{\mu}\tilde{u}_{k,k}\delta_{ij} + \overline{\mu}(\tilde{u}_{i,j} + \tilde{u}_{j,i}) \tag{13}$$

$$\overline{\rho}\varepsilon = \overline{\sigma_{ij}' u_{i,j}'} \tag{14}$$

are, respectively, the Reynolds stress tensor, the Reynolds heat flux, the mean viscous stress tensor, and the turbulent dissipation rate. Eqs. (8) - (10) are derived subject to one major assumption: turbulent fluctuations in the viscosity, thermal conductivity and specific heat can be neglected.

The pressure gradient-velocity correlation $\overline{u_i' p_{,i}'}$ can be written in the equivalent form (see Speziale and Sarkar[13])

$$\overline{u_i' p_{,i}'} = -(\overline{\rho} R \tilde{T} \overline{u_i''})_{,i} + (\overline{\rho} R \widetilde{u_i'' T''})_{,i} - \overline{p' u_{i,i}'} \; . \tag{15}$$

Consequently, in order to achieve closure, models are needed for: (a) the Reynolds stress τ_{ij}, (b) the Reynolds heat flux Q_i, (c) the turbulent dissipation rate ε, (d) the pressure dilatation correlation $\overline{p' u_{i,i}'}$ and (e) the mass flux $\overline{u_i''}$. Consistent with the recent work of Sarkar et al.[9], the dissipation is decomposed into solenoidal and compressible parts:

$$\varepsilon = \varepsilon_s + \varepsilon_c \tag{16}$$

where for homogeneous turbulence $\overline{\rho}\varepsilon_s = \overline{\mu\omega_i'\omega_i'}$ and $\overline{\rho}\varepsilon_c = \frac{4}{3}\overline{\mu(u_{i,i}')^2}$ given that ω_i' is the fluctuating vorticity. Here, ε_s represents the dissipation associated with the energy cascade. The length and time scales will be built up from ε_s which is to be obtained from a modeled transport equation. The Sarkar et al.[9] model for the compressible dissipation will be used in the form:

$$\varepsilon_c = \alpha M_t^2 \varepsilon_s \tag{17}$$

where $M_t = (\widetilde{u_i''u_i''}/\gamma R\tilde{T})^{\frac{1}{2}}$ is the turbulence Mach number given that $\gamma = \overline{C}_p/\overline{C}_v$ is the ratio of specific heats. Here, the constant α is approximately 0.5 based on direct numerical simulations of homogeneous shear flow[10].

The Reynolds stress tensor is modeled in the standard eddy viscosity form

$$\tau_{ij} = \frac{2}{3}K\delta_{ij} - 2C_\mu f_\mu \frac{K^2}{\varepsilon_s}(\tilde{S}_{ij} - \frac{1}{3}\tilde{S}_{kk}\delta_{ij}) \tag{18}$$

where $K = \frac{1}{2}\tau_{ii}$ is the turbulent kinetic energy, $\tilde{S}_{ij} = \frac{1}{2}(\partial\tilde{u}_i/\partial x_j + \partial\tilde{u}_j/\partial x_i)$ is the Favre-averaged rate of strain tensor, C_μ is a dimensionless constant taken to be 0.096, and f_μ is a wall damping function. The wall damping function f_μ – which goes to one sufficiently far from the wall – will be discussed in more detail later. A simple eddy viscosity model was chosen since we are dealing with two-dimensional attached boundary layers; for other applications involving more complex flows, (18) can be easily generalized to an algebraic stress model or an anisotropic eddy viscosity model (see Rodi[14] and Speziale[15]).

The Reynolds heat flux and mass flux terms are modeled by the standard gradient transport hypotheses:

$$\widetilde{u_i''T''} = -\frac{C_\mu f_\mu}{Pr_T}\frac{K^2}{\varepsilon_s}\tilde{T}_{,i} \tag{19}$$

$$\overline{u_i''} = \frac{C_\mu f_\mu}{\overline{\rho}\sigma_\rho}\frac{K^2}{\varepsilon_s}\overline{\rho}_{,i} \tag{20}$$

where Pr_T is the turbulent Prandtl number which is taken to be 0.9 and σ_ρ is the mass flux constant which assumes a value of 0.5. A recently derived model by Sarkar[10] is used for the pressure dilatation correlation which is given by

$$\overline{p'u_{i,i}'} = -\alpha_1\overline{\rho}\mathcal{P}M_t^2 + \alpha_2\overline{\rho}\varepsilon_s M_t^2 \tag{21}$$

where $\mathcal{P} = -\tau_{ij}\tilde{u}_{i,j}$ is the turbulence production. Based on direct numerical simulations of homogeneous shear flow, Sarkar[10] determined that $\alpha_1 \approx 0.4$ and $\alpha_2 \approx 0.2$.

In order to achieve closure, modeled transport equations for the turbulent kinetic energy K and the solenoidal part of the turbulent dissipation rate ε_s are needed. The exact transport

equation for the turbulent kinetic energy is given by[13]

$$\frac{\partial}{\partial t}(\overline{\rho}K) + (\overline{\rho}\tilde{u}_i K)_{,i} = -\overline{\rho}\tau_{ij}\tilde{u}_{i,j} - \overline{\rho}\varepsilon + \overline{p'u'_{i,i}} - \overline{u''_i}\overline{p}_{,i} + \overline{u''_i}\overline{\sigma}_{ij,j} + \mathcal{D}^T_{i,i} + \mathcal{D}^M_{i,i} \tag{22}$$

where

$$\mathcal{D}^T_i = -\frac{1}{2}\overline{\rho}\widetilde{u''_i u''_j}u''_j - \overline{p'u'_i}, \quad \mathcal{D}^M_i = \overline{u'_k\sigma'_{ki}} \tag{23}$$

are, respectively, the turbulent and molecular diffusion terms. If turbulent fluctuations in the viscosity are neglected, as well as other higher-order terms, the molecular diffusion can be approximated as

$$\mathcal{D}^M_i = \overline{\mu}K_{,i} \tag{24}$$

in the boundary layer. Formally, (24) is the leading order part of (23) close to the wall provided that turbulent fluctuations in the viscosity and density can be neglected. The standard gradient transport hypothesis is applied to the modeling of the turbulent diffusion term:

$$\mathcal{D}^T_i = \frac{\mu_T}{\sigma_K}K_{,i} \tag{25}$$

where again $\mu_T = \overline{\rho}C_\mu f_\mu K^2/\varepsilon_s$ is the eddy viscosity and σ_K is a constant taken to be 0.75. This leads to the final modeled transport equation for K:

$$\begin{aligned}\frac{\partial}{\partial t}(\overline{\rho}K) + (\overline{\rho}\tilde{u}_i K)_{,i} &= -\overline{\rho}\tau_{ij}\tilde{u}_{i,j} - \overline{\rho}(1+\alpha M_t^2)\varepsilon_s - \alpha_1\overline{\rho}\mathcal{P}M_t^2 \\ &\quad +\alpha_2\overline{\rho}\varepsilon_s M_t^2 - \overline{u''_i}\overline{p}_{,i} + \overline{u''_i}\overline{\sigma}_{ij,j} + \left[\left(\overline{\mu} + \frac{\mu_T}{\sigma_K}\right)K_{,i}\right]_{,i}\end{aligned} \tag{26}$$

The exact transport equation for the solenoidal part of the turbulent dissipation rate is of the general form:

$$\frac{\partial}{\partial t}(\overline{\rho}\varepsilon_s) + (\overline{\rho}\tilde{u}_i\varepsilon_s)_{,i} = -\frac{4}{3}\overline{\rho}\varepsilon_s\tilde{u}_{i,i} + \overline{\rho}\varepsilon_s\frac{1}{\overline{\nu}}\frac{D\overline{\nu}}{Dt} + \mathcal{P}_{\varepsilon_s} - \Phi_{\varepsilon_s} + \mathcal{D}_{\varepsilon_s} + (\overline{\mu}\varepsilon_{s,i})_{,i} \tag{27}$$

where $\mathcal{P}_{\varepsilon_s}$ is the production of solenoidal dissipation, Φ_{ε_s} is the corresponding destruction term, and $\mathcal{D}_{\varepsilon_s}$ is the turbulent diffusion of solenoidal dissipation. For the sake of brevity, the details of the higher-order correlations that comprise $\mathcal{P}_{\varepsilon_s}, \Phi_{\varepsilon_s}$ and $\mathcal{D}_{\varepsilon_s}$ are not given (these correlations are quite complicated). In deriving the viscous term in (27), turbulent fluctuations in the molecular viscosity have been neglected consistent with the earlier derivations. The term $\mathcal{P}_{\varepsilon_s}$ in (27) represents the production of solenoidal dissipation by deviatoric mean strains as well as by density fluctuations. This term will be modeled as a variable density extension of its incompressible form with density fluctuations neglected[13]. Hence, we take

$$\mathcal{P}_{\varepsilon_s} = -C_{\varepsilon 1}\overline{\rho}\frac{\varepsilon_s}{K}\tau_{ij}(\tilde{u}_{i,j} - \frac{1}{3}\tilde{u}_{k,k}\delta_{ij}) \tag{28}$$

where $C_{\varepsilon 1}$ is a dimensionless constant taken to be 1.5. The same approach is used in the modeling of the destruction term which yields

$$\Phi_{\varepsilon_s} = C_{\varepsilon 2} f_2 \overline{\rho} \frac{\varepsilon_s^2}{K} \tag{29}$$

where f_2 is a wall damping function and $C_{\varepsilon 2}$ is a dimensionless constant which is taken to be 1.83. The standard gradient transport hypothesis is used for the turbulent diffusion term $\mathcal{D}_{\varepsilon_s}$:

$$\mathcal{D}_{\varepsilon_s} = \left(\frac{\mu_T}{\sigma_\varepsilon} \varepsilon_{s,i} \right)_{,i} \tag{30}$$

where σ_ε is a dimensionless constant which is taken to be 1.45.

Modeling the variable viscosity term in (27) is a bit trickier. For the high Mach number flows to be considered in this paper, variations of the viscosity with temperature must be accounted for. In this vain, we use Sutherland's law[16] for which

$$\overline{\mu} = \overline{\mu}_0 \left(\frac{\tilde{T}}{\tilde{T}_0} \right)^{\frac{1}{2}} \left(\frac{1 + \chi/\tilde{T}_0}{1 + \chi/\tilde{T}} \right) \tag{31}$$

where $\tilde{T}_0$ and $\overline{\mu}_0$ are the reference temperature and viscosity whereas χ is a constant that depends on the gas (for air, $\chi = 110°K$). Eq. (31) could also be used for the viscosity transport term $(1/\overline{\nu})D\overline{\nu}/Dt$ in (27). However, this would couple the dissipation rate transport equation to the continuity and energy equations at the highest time derivative – an undesirable feature that can cause numerical stiffness. Hence, following the work of Coleman and Mansour[11], we will use the power law approximation

$$\overline{\mu} = \overline{\mu}_0 \left(\frac{\tilde{T}}{\tilde{T}_0} \right)^n, \tag{32}$$

(where $n \approx 0.7$) for the formulation of the viscosity transport term $(1/\overline{\nu})D\overline{\nu}/Dt$ in (27); Sutherland's law will, however, be used for the calculation of the viscous diffusion terms since it is more accurate. Coleman and Mansour[11] showed that, for an isentropic compression, (32) yields the relation

$$\frac{1}{\overline{\nu}} \frac{D\overline{\nu}}{Dt} = [1 - n(\gamma - 1)] \tilde{u}_{i,i} \tag{33}$$

where $\gamma = \overline{C}_p/\overline{C}_v$ is the ratio of specific heats. On physical grounds one would expect (33) to constitute the leading order part of $(1/\overline{\nu})D\overline{\nu}/Dt$ and it will be used to avoid numerical stiffness problems. The final form of the modeled dissipation rate equation is obtained by

substituting (28) - (33) into (27) which yields

$$\frac{\partial}{\partial t}(\overline{\rho}\varepsilon_s) + (\overline{\rho}\tilde{u}_i\varepsilon_s)_{,i} = -\left[\frac{1}{3} + n(\gamma-1)\right]\overline{\rho}\varepsilon_s\tilde{u}_{i,i} - C_{\varepsilon 1}\overline{\rho}\frac{\varepsilon_s}{K}\tau_{ij}\left(\tilde{u}_{i,j} - \frac{1}{3}\tilde{u}_{k,k}\delta_{ij}\right) - C_{\varepsilon 2}f_2\overline{\rho}\frac{\varepsilon_s^2}{K} + \left[\left(\overline{\mu} + \frac{\mu_T}{\sigma_\varepsilon}\right)\varepsilon_{s,i}\right]_{,i} \tag{34}$$

where $n \approx 0.7$. The mean viscosity $\overline{\mu}$ is approximated by Sutherland's law in (34) as well as in the other transport equations.

3. NEAR WALL MODIFICATIONS FOR COMPRESSIBLE FLOWS

Now we will address the issue of near-wall modeling in more detail. Two fundamental assumptions will be made: (i) the functions are analytic so that they can be expanded in a Taylor series near the wall, and (ii) turbulent fluctuations of the density and temperature vanish at the wall. While the former assumption is well accepted, the latter one – despite its widespread use – is somewhat debatable. However, since this assumption is rigorously valid for isothermal wall conditions – and a good approximation for the adiabatic wall – we are justified in using this simplification for the present paper. Without this assumption, the near wall asymptotics become much more uncertain.

A Taylor expansion then yields:

$$\rho' = \beta_1 y + \beta_2 y^2 + \cdots \tag{35}$$

$$T'' = \gamma_1 y + \gamma_2 y^2 + \cdots \tag{36}$$

where β_i and γ_i are functions of x, z and t given that y is the coordinate normal to the wall. Due to (35) and the continuity equation (1), it follows that the fluctuating velocity components (u, v, w) have the expansions

$$u = a_1 y + a_2 y^2 + \cdots \tag{37}$$

$$v = b_2 y^2 + b_3 y^3 + \cdots \tag{38}$$

$$w = c_1 y + c_2 y^2 + \cdots \tag{39}$$

near the wall based on either standard or Favre averages. Equations (37) - (39) are identical to their incompressible counterparts – a simplification that arises from the assumption of vanishing density fluctuations at the wall. By using (37) - (39), it is straightforward to show that we have the following near-wall asymptotics for the crucial turbulence correlations:

$$K = \mathcal{O}(y^2), \quad \varepsilon_s = \mathcal{O}(1), \quad \varepsilon_c = \mathcal{O}(y^2) \tag{40}$$

$$\mu_T = \mathcal{O}(y^3), \quad \overline{p' u'_{i,i}} = \mathcal{O}(y^2) \tag{41}$$

$$(\widetilde{u''_i T''})_{,i} = \mathcal{O}(y^2), \quad (\overline{u''_i})_{,i} = \mathcal{O}(y^2) \tag{42}$$

$$\mathcal{P}_{\varepsilon_s} = \mathcal{O}(y), \quad \Phi_{\varepsilon_s} = \mathcal{O}(1) \tag{43}$$

(the precise asymptotic behavior of the turbulent diffusion terms (25) and (30) are not of consequence since they constitute higher-order terms near the wall). The asymptotic constraints (40) - (43) can be satisfied identically with only two damping functions, f_μ and f_2, which behave as

$$f_\mu = \mathcal{O}(y^{-1}), \quad f_2 = \mathcal{O}(y^2) \tag{44}$$

near the wall.

Consistent with the underlying assumption that the density fluctuations vanish at the wall – which renders the fluctuating velocity to be solenoidal to the leading order near the wall – a variable density extension of the incompressible wall damping functions of So et al.[8] will be used. Validations of these wall damping functions have been carried out for a number of two-dimensional flows, including internal and external flows as well as flows with heat transfer[17–19]. In all of these cases, good correlations with direct simulation data[20–24] and measurements[25] have been obtained. These wall damping functions are implemented in the form:

$$f_\mu = \left(1 + \frac{3.45}{\sqrt{R_t}}\right) \tanh(y^+/115) \tag{45}$$

$$f_2 = \frac{\tilde{\varepsilon}_s}{\varepsilon_s}\left[1 + \frac{2 f_{w2}}{C_{\varepsilon 2}} - \frac{3}{2}\frac{f_{w2}}{C_{\varepsilon 2}}\left(\frac{\varepsilon_s^{*2}}{\varepsilon_s \tilde{\varepsilon}_s}\right)\right] \tag{46}$$

where

$$y^+ = y u_\tau / \overline{\nu} \tag{47}$$

$$f_{w2} = e^{-(R_t/64)^2}, \quad R_t = K^2/\overline{\nu}\varepsilon_s \tag{48}$$

$$\varepsilon_s^* = \varepsilon_s - 2\overline{\nu} K / y^2 \tag{49}$$

$$\tilde{\varepsilon}_s = \varepsilon_s - 2\overline{\nu}(\sqrt{K})_{,i}(\sqrt{K})_{,i} \tag{50}$$

In (47) - (50), $\overline{\nu} = \overline{\mu}/\overline{\rho}$ is the local mean kinematic viscosity and u_τ is the friction velocity defined by

$$u_\tau = \sqrt{\tau_w / \overline{\rho}_w}. \tag{51}$$

where τ_w is the wall shear stress[26].

4. THE FLAT-PLATE BOUNDARY LAYER EQUATIONS

The steady boundary layer form of the mean turbulence equations corresponding to this model are now provided. Consistent with most practical computations of compressible flows[27], we will solve the energy equation in its total enthalpy form where

$$\tilde{H} = \overline{C}_p \tilde{T} + \frac{1}{2}\tilde{u}_i\tilde{u}_i + K \tag{52}$$

is the Favre-averaged total enthalpy. The resulting boundary layer equations at zero pressure gradient take the form:

$$\frac{\partial}{\partial x}(\overline{\rho}\tilde{u}) + \frac{\partial}{\partial y}(\overline{\rho}\tilde{v}) = 0 \tag{53}$$

$$\overline{\rho}\tilde{u}\frac{\partial \tilde{u}}{\partial x} + \overline{\rho}\tilde{v}\frac{\partial \tilde{u}}{\partial y} = \frac{\partial}{\partial y}\left[(\overline{\mu} + \mu_T)\frac{\partial \tilde{u}}{\partial y}\right] \tag{54}$$

$$\overline{\rho}\tilde{u}\frac{\partial \tilde{H}}{\partial x} + \overline{\rho}\tilde{v}\frac{\partial \tilde{H}}{\partial y} = \frac{\partial}{\partial y}\left\{\left(\frac{\overline{\mu}}{Pr} + \frac{\mu_T}{Pr_T}\right)\frac{\partial \tilde{H}}{\partial y} + \left[\overline{\mu}\left(1 - \frac{1}{Pr}\right) + \mu_T\left(1 - \frac{1}{Pr_T}\right)\right]\tilde{u}\frac{\partial \tilde{u}}{\partial y} + \left[\overline{\mu}\left(1 - \frac{1}{Pr}\right) + \mu_T\left(\frac{1}{\sigma_K} - \frac{1}{Pr_T}\right)\right]\frac{\partial K}{\partial y}\right\} \tag{55}$$

$$\overline{\rho}\tilde{u}\frac{\partial K}{\partial x} + \overline{\rho}\tilde{v}\frac{\partial K}{\partial y} = \mu_T\left(\frac{\partial \tilde{u}}{\partial y}\right)^2 - \overline{\rho}(1 + \alpha M_t^2)\varepsilon_s - \alpha_1\mu_T\left(\frac{\partial \tilde{u}}{\partial y}\right)^2 M_t^2 + \alpha_2\overline{\rho}\varepsilon_s M_t^2 + \overline{u''}\frac{\partial}{\partial y}\left(\overline{\mu}\frac{\partial \tilde{u}}{\partial y}\right) + \frac{\partial}{\partial y}\left[\left(\overline{\mu} + \frac{\mu_T}{\sigma_K}\right)\frac{\partial K}{\partial y}\right] \tag{56}$$

$$\overline{\rho}\tilde{u}\frac{\partial \varepsilon_s}{\partial x} + \overline{\rho}\tilde{v}\frac{\partial \varepsilon_s}{\partial y} = -\left[\frac{1}{3} + n(\gamma - 1)\right]\overline{\rho}\left(\frac{\partial \tilde{u}}{\partial x} + \frac{\partial \tilde{v}}{\partial y}\right)\varepsilon_s - C_{\varepsilon 1}\frac{\varepsilon_s}{K}\mu_T\left(\frac{\partial \tilde{u}}{\partial y}\right)^2 - C_{\varepsilon 2}f_2\overline{\rho}\frac{\varepsilon_s^2}{K} + \frac{\partial}{\partial y}\left[\left(\overline{\mu} + \frac{\mu_T}{\sigma_\varepsilon}\right)\frac{\partial \varepsilon_s}{\partial y}\right] \tag{57}$$

where $\mu_T = \overline{\rho}C_\mu f_\mu K^2/\varepsilon_s$ is the turbulent viscosity. A summary of the values of the constants is given as follows: $C_\mu = 0.096$, $C_{\varepsilon 1} = 1.5$, $C_{\varepsilon 2} = 1.83$, $\sigma_K = 0.75$, $\sigma_\varepsilon = 1.45$, $\sigma_\rho = 0.5$, $\alpha = 0.5$, $\alpha_1 = 0.4$, $\alpha_2 = 0.2$, and $n = 0.7$. The damping functions are as specified in (45) - (46); consequently, the two equation model of So et al.[8] is recovered in the incompressible limit. The turbulent Prandtl number Pr_T is specified as 0.9; the molecular Prandtl number Pr is taken to be 0.74 for air and 0.70 for helium; and the specific heat ratio γ is 1.4 for air and 1.67 for helium. Sutherland's law (31) is used to evaluate the molecular viscosity in (54) - (57) for air; for helium the power law quoted in Fernholz and Finley[28] is used.

A few comments are in order concerning the derivation of the transport equation for the total enthalpy $\tilde{H}$. We obtain this equation by adding the modeled transport equations for $\overline{C}_p\tilde{T}$, $\frac{1}{2}\tilde{u}_i\tilde{u}_i$ and K. As an alternative approach, the exact transport equation for $\tilde{H}$ can be modeled directly. However, we do not feel that this is a good approach since $\tilde{H}$ is not a Galilean invariant quantity.

Equations (53) - (57) are solved subject to the standard boundary conditions:

$$\tilde{u} = 0,\ \tilde{v} = 0,\ K = 0,\ \varepsilon_s = 2\overline{\nu}_w(\partial\sqrt{K}/\partial y)^2 \tag{58}$$

at the wall. Two different types of thermal wall boundary conditions will be considered: the adiabatic wall where $\partial\tilde{H}/\partial y$ is zero and the cooled wall case where $\tilde{H}$ is constant. At the edge of the boundary layer, the mean velocity and the total enthalpy are required to match the specified free-stream conditions. On the other hand, the turbulence quantities, K and ε_s, are assumed to be zero in the free stream. Thus formulated, the above equations with the appropriate boundary conditions can be solved numerically using the boundary-layer code developed by Anderson and Lewis[27] and modified by So et al.[8]

5. DISCUSSION OF RESULTS

Two versions of the $K-\varepsilon$ model derived herein are used to carry out the compressible flat plate boundary-layer calculations to be presented in this section. One version consists of the full compressible model as given in Eqs. (53) - (57) and is designated as $K-\varepsilon$ model/1. The second version – which is designated as $K-\varepsilon$ model/2 – is a variable density extension of the incompressible two-equation model of Reference 8 wherein the explicit compressible terms in (56) and (57) are neglected along with the $\partial K/\partial y$ term in (55). Furthermore, comparisons will also be made with results of the well-known $K-\omega$ model of Wilcox[12]. The calculations of these two different versions of the new $K-\varepsilon$ model, as well as those for the $K-\omega$ model, will allow us to evaluate the range of validity of Morkovin's hypothesis and assess the importance of having an asymptotically consistent near-wall correction for turbulence models. Therefore, the central questions posed in the Introduction can be addressed by comparing these results with well-documented experimental data spanning a wide range of free-stream Mach numbers and cooled wall conditions.

The three different models mentioned above are used to calculate compressible flat plate boundary layers on adiabatic as well as cooled walls and the results are compared with measurements drawn from References 28 and 29. The calculations are carried out over the Mach number range $0 < M_\infty < 10$ for the adiabatic wall boundary condition and over the temperature range, $0 < T_\infty/T_{aw} < 1$ for the cooled wall case. Here, M_∞ is the free-stream Mach number, T_∞ is the free-stream temperature and T_{aw} is the adiabatic wall temperature.

Since only mean flow properties are available from Reference 28, comparisons are made with these measured quantities only and the reported skin friction coefficient, $C_f = 2\tau_w/\overline{\rho}_\infty U_\infty^2$ (where U_∞ is the free-stream velocity and $\overline{\rho}_\infty$ is the free-stream mean density). In addition, comparisons of the calculated turbulence quantities are made with the results of the $K-\omega$ model. All calculations are carried out to the same momentum thickness Reynolds number (R_θ) as the measurements and the comparisons are made at these respective locations. Four sets of data are chosen from Reference 28. These are cases 55010504, 53011302, and 73050504 with the adiabatic wall boundary condition and case 59020105 with a constant cooled wall temperature. M_∞ for these cases are 2.244, 4.544, 10.31, and 5.29, respectively, and the corresponding values of R_θ are: 20,797; 5,532; 15,074; and 3,939. The variations of C_f with M_∞ and T_∞/T_{aw} are compared with the van Driest II results given in Reference 29. Finally, the mean velocity profiles are compared with the van Driest law-of-the-wall for compressible boundary layers[30,31] and an assessment of the effects of compressibility on boundary-layer flows is attempted.

The mean velocities are presented in two different forms: one in terms of wall variables, u^+ versus $ln\ y^+$, and another in terms of outer variables, $\tilde{u}/U_\infty$ versus y/δ. Here, $u^+ = \tilde{u}/u_\tau$, $y_w^+ = yu_\tau/\overline{\nu}_w$ and δ is the boundary-layer thickness. In this way, the effects of the calculated u_τ and $\overline{\rho}$ on the mean velocities can be assessed. The mean temperature is plotted in the form of $\tilde{T}/T_\infty$ versus y/δ while all turbulence quantities, such as K and $-\overline{uv}$, are normalized by u_τ^2 to give k^+ and $-\overline{uv}^+$, respectively, for presentation. A comparison with the van Driest law-of-the-wall[30,31] for compressible flows is also attempted; therefore, the mean velocities of two cases are plotted in terms of the compressible u^+ defined according to Reference 31 as $u_c^+ = \int_0^{u^+} (\overline{\rho}/\overline{\rho}_w)^{\frac{1}{2}}\, du^+$. Since the K budgets for all cases considered are essentially similar, only the budget of K in the near-wall region for case 73050504 ($M_\infty = 10.31$ and $T_w/T_r = 1.0$) is presented. Here, the reference temperature T_r is taken to be the recovery temperature for the cases with an adiabatic wall boundary condition and taken to be the adiabatic wall temperature for the cooled-wall case.

The u^+ versus $ln\ y_w^+$ plots for the four cases are shown in Figures 1 and 2. In each figure, the calculated and measured skin friction coefficient C_f, as well as that determined from the van Driest II formula of Reference 29, are listed for comparison. A standard law-of-the-wall given by $u^+ = (1/\kappa) ln\ y_w^+ + B$ is also shown for comparison, where the von Karman constant $\kappa = 0.41$ has been assumed. It is recognized that the intercept B should be a function of M_∞, however, in these figures, B is taken to be 4.7. The actual value used here is not too important because the objective is to determine and compare the variation, if any, of the log-law slope with M_∞ and T_w/T_r. The log-law is seen to hold true for all cases calculated using both the $K-\varepsilon$ and $K-\omega$ models (Figures 1 and 2) and the value of κ thus determined

for the three adiabatic wall cases is essentially 0.41. For the cooled-wall case, the calculated κ is not equal to 0.41 and varies from model to model. The best agreement with data is given by the calculation using $K-\varepsilon$ model/2 while the smallest value of κ is predicted by the $K-\omega$ model. All models considered yield calculations of C_f that are in agreement with measured data and with van Driest II values. The maximum error is less than 4% (Figures 1 and 2). An exception is the cooled-wall case where the measurement is higher than the van Driest II value. According to Reference 28, the measured C_f in this case is not as accurate as in the other cases and this explains the discrepancy between the calculated and measured C_f shown in Figure 2. This comparison, therefore, shows that the additional compressible terms in the governing equations do not significantly affect the calculated results so long as the near-wall model used is the same and is asymptotically consistent. In other words, Morkovin's hypothesis is valid for flows with free-stream Mach numbers as high as 10 and wall temperature ratios noticeably smaller than one.

In the past, velocity profiles in wall coordinates were invariably plotted in terms of u_c^+ to illustrate the existence of the van Driest log-law and the constancy of κ in compressible boundary-layer flows[6,30,31]. Since then, the compressible law of the wall is typically taken to be given by u_c^+ rather than by u^+, and κ is considered to be about 0.41 and constant over the Mach number range of $0 \leq M_\infty \leq 5$. The calculated and measured velocity plots given in Figures 1 and 2 show support for the compressible law-of-the-wall when it is written in terms of u^+ rather than u_c^+. Furthermore, κ is determined to be approximately 0.41 and is relatively constant over the Mach number range of 0 - 10 for the adiabatic wall boundary condition. These results seem to conflict with the proposal of van Driest[30]. In order to resolve this seeming contradiction, the velocity plots of u_c^+ versus $ln\ y_w^+$ for cases 55010504 ($M_\infty = 2.244, T_w/T_r = 1$) and 53011302 ($M_\infty = 4.544, T_w/T_r = 1$) are shown in Figure 3. In addition, the compressible law-of-the-wall as given in Reference 31 is shown for comparison. It can be seen that a line that is parallel to the compressible law-of-the-wall can be drawn through a few of the data points spanning over a narrow range of y_w^+. On the other hand, the calculated profiles are in agreement with data over a wider range of y_w^+. The slopes of the calculated profiles are roughly parallel to that determined from measurements and are slightly larger than the slope of the compressible law-of-the-wall shown. Therefore, irrespective of how the velocity profiles are plotted, the calculations are in good agreement with data. However, the slope of the log-law appears to be given by $(0.41)^{-1}$ only when the profiles are plotted in terms of u^+.

Based on the above comparisons, it seems that there is very little difference between the predictions of the $K-\varepsilon$ and $K-\omega$ models. This is particularly true in regard to the calculations of C_f. The semi-log plots shown in Figure 1 tend to mask the differences found

between the models in the calculations of the mean temperature and density profiles. These differences begin to show up in the plots shown in Figure 3 and in the predictions of the cooled-wall case (Figure 2). In order to determine the actual difference between the mean flow predictions of the $K-\varepsilon$ and $K-\omega$ models, plots of $\tilde{u}/U_\infty$ versus y/δ are given in Figures 4 and 5 for the adiabatic and cooled wall conditions, respectively, while the corresponding mean temperature profiles are plotted in Figures 6 and 7. These results show that there are substantial discrepancies between measurements and the profiles of $\tilde{u}/U_\infty$ and $\tilde{T}/T_\infty$ calculated using the $K-\omega$ model. The discrepancies increase as M_∞ increases and as T_w/T_r decreases. The best results are given by $K-\varepsilon$ model/1. On the other hand, the predictions of $K-\varepsilon$ model/2 are very close to those of $K-\varepsilon$ model/1 and are substantially different from those of the $K-\omega$ model. This is further evidence that an asymptotically consistent near-wall model is more important than the additional compressible terms as far as the predictions of the mean flow properties are concerned.

The ability of the $K-\omega$ model to predict the variations of C_f with M_∞ and T_w/T_{aw} is well established[12]. If the proposed $K-\varepsilon$ model is to be accepted, its ability to predict C_f for different M_∞ and T_w/T_{aw} has to be demonstrated. In Figure 8, the variation of $C_f/(C_f)_i$ with M_∞ for the case of the adiabatic wall boundary condition is shown. Here, $(C_f)_i$ is the skin friction coefficient for an incompressible flow evaluated at $R_\theta = 10^4$ which is determined to be 2.70×10^{-3}. This figure shows a comparison of the calculations of $K-\varepsilon$ model/1 and $K-\varepsilon$ model/2 with the van Driest II curve[29]. Essentially, there is no difference between the predictions of $K-\varepsilon$ model/1 and $K-\varepsilon$ model/2 and both results are in excellent agreement with data. The predictions for the cooled wall case are shown in Figure 9. Calculations for this case are carried out for $M_\infty = 5$ and $R_\theta = 10^4$ where the incompressible C_f is again determined to be 2.70×10^{-3}. Three sets of calculations are presented. These are for $K-\varepsilon$ model/1, $K-\varepsilon$ model/2 and a third version of $K-\varepsilon$ model/1 where the $\partial K/\partial y$ term in (56) is neglected. It can be seen that an error of 5% or larger starts to accumulate at approximately $T_w/T_{aw} = 0.4$ for $K-\varepsilon$ model/1. This trend is contrary to the results reported in Reference 12. An examination of the governing equations solved by other researchers revealed that, besides the differences noted in the turbulence model equations, the mean enthalpy equation solved by these researchers does not include the term $\partial K/\partial y$ on the right hand side of (55). Indeed, when the $\partial K/\partial y$ term is neglected, an overall important improvement is obtained. The predicted C_f at $T_w/T_{aw} = 0.2$ is increased by about 6%, thus giving a much better agreement with the van Driest II curve[29]. If the additional compressible terms in the $K-\varepsilon$ equations are further neglected ($K-\varepsilon$ model/2), the calculated C_f is only improved by about 2%. The remaining disagreement could be attributed to the assumption of a constant turbulent Prandtl number which cannot properly account for a reduction of turbulent mixing

resulting from a cooled wall (in fact, the $\partial K/\partial y$ term can be formally dropped if $Pr_T = 0.74$; such a lowering of the turbulent Prandtl number would not be inconsistent with experiments for the cooled wall case). However, this effect can be appropriately incorporated in a heat-flux model and modifications can be formulated to describe its near-wall behavior[19,32]. In other words, if highly cooled-wall flows are to be predicted correctly, turbulent heat fluxes and their near-wall behavior need to be modeled.

The distributions of k^+ and $-\overline{uv}^+$ across the boundary layers are compared in Figures 10 - 13. In these figures, only the results of $K-\varepsilon$ model/1 and the $K-\omega$ model are compared. The results for the adiabatic wall boundary condition are shown in Figures 10 and 12 while those for the cooled-wall case are plotted in Figures 11 and 13. It can be seen that the $K-\omega$ model underpredicts k^+ in the near-wall region and overestimates its value in the outer part of the boundary layer. This incorrect prediction is common for all cases studied. The predicted near-wall behavior is substantially different from that given by $K-\varepsilon$ model/1. Instead of yielding a finite slope for k^+ at the wall, a near zero slope is calculated. Furthermore, the maximum k^+ calculated is about half that given by $K-\varepsilon$ model/1. On the other hand, the $K-\omega$ model yields the correct near-wall behavior for $-\overline{uv}^+$ but overpredicts its value in the outer part of the boundary layer. The overprediction extends across the range, $0.2 \leq y/\delta \leq 1.0$. It is now clear that the $K-\omega$ model is formulated to give correct results for the mean velocity and the wall shear stress; however, its predictions of other properties are in doubt, particularly, in regard to the near-wall behavior. Reduction of turbulence activity in the outer part of the boundary layer is clearly evident when either compressibility or wall cooling effects are present. The reduction increases as M_∞ increases and T_w/T_r decreases. This is further substantiated by the very significant drop in the maximum value of k^+ as M_∞ increases. Therefore, it is expected that turbulence activity will be substantially reduced in a flow where the free-stream Mach number is large and the wall is highly cooled.

The predictions of the near-wall flow can be further examined. With the assumption of vanishing ρ' and T'' at the wall, Taylor expansions of the fluctuating velocities, density and temperature about $y = 0$ are given by (35) - (39). These expansions together with the definition for ε_s can be rearranged to give the following dimensionless expansions for k^+, $-\overline{uv}^+$ and ε_s^+, i.e.,

$$k^+ = a_k(y_w^+)^2 + b_k(y_w^+)^3 + \ldots, \tag{59}$$

$$-\overline{uv}^+ = a_{uv}(y_w^+)^3 + b_{uv}(y_w^+)^4 + \ldots, \tag{60}$$

$$\varepsilon_s^+ = 2a_k + 4b_k y_w^+ + \ldots, \tag{61}$$

where the a's and b's are time-averaged coefficients that are functions of x and z. From these expansions, it can be easily deduced that $k^+/\varepsilon_s^+(y_w^+)^2 = 0.5$ at the wall. Therefore, the

asymptotic behavior of $k^+/\varepsilon_s^+(y_w^+)^2$ is 0.5 and is independent of M_∞ as well as the thermal wall boundary conditions. The accuracy to which a model can predict this quantity is a reflection of its asymptotic consistency. Finally, the variation of ε_s^+ at the wall with Mach number can be deduced from a plot of a_k versus M_∞; therefore, this result is shown in Figure 14 for the cases with the adiabatic wall boundary condition. The value of a_k for the corresponding incompressible flow is taken from Reference 8. Model calculations of a_k, a_{uv} and $k^+/\varepsilon_s^+(y_w^+)^2$ are tabulated in Table 1 for comparison. Since the $K-\omega$ model is not an asymptotically consistent near-wall model, its predictions of these limiting values are poor; therefore, they are not listed in Table 1. From these results, it can be seen that the present $K-\varepsilon$ model is asymptotically consistent up to a Mach number M_∞ of 10 for both adiabatic and cooled wall conditions. In other words, the predictions of k^+ and $-\overline{uv}^+$ shown in Figures 10 - 13 are more likely to be correct compared to those given by the $K-\omega$ model. These results further show that a_k is a function of the Mach number and decreases with increasing M_∞ (see Figure 14). This means that viscous dissipation at the wall also decreases with increasing M_∞.

The near-wall budget of K for the $M_\infty = 10.31$ case (73050504) is shown in Figure 15. It is evident that the budget of K bears a strong resemblence to that calculated for incompressible flows[17]. The additional compressible terms have a negligible effect on the near-wall K budget. Therefore, the assumptions made to extend the near-wall damping function f_2 in the dissipation-rate equation to compressible flows appear to be justified. Again, it can be seen that viscous diffusion balances dissipation at the wall. This balance extends to about $y_w^+ = 4$ where turbulent diffusion and production become important. In the region, $4 \leq y_w^+ \leq 15$, viscous and turbulent diffusion as well as production and dissipation are equally important. Beyond $y_w^+ = 15$, production and dissipation are approximately in balance, just as in the case of incompressible flows. Consequently, the near-wall behavior of K is very similar for both incompressible and compressible flows (thus, explicit compressibility effects are not that important in the near-wall region).

6. CONCLUSIONS

In contrast to the conclusions drawn by Bradshaw et al.[5] and Huang et al.[6], the present investigation shows that conventional $K-\varepsilon$ models can be extended to calculate equilibrium compressible boundary-layers, at high Mach numbers, if the near-wall modifications to these models are asymptotically correct and internally consistent. When properly modified, $K-\varepsilon$ type models can be used to calculate equilibrium compressible boundary-layers with free-stream Mach numbers as high as 10 and wall temperature ratios as low as 0.2. Two different versions of the $K-\varepsilon$ model proposed in this study are tested: one with all of

the systematically derived dilatational terms included in the governing equations ($K-\varepsilon$ model/1) and another which is a variable density extension of the incompressible limit of this model where explicit compressible terms are neglected ($K-\varepsilon$ model/2). Calculated mean flow properties and wall shear stresses from these two versions of the $K-\varepsilon$ model are in excellent agreement with measurements. The near-wall behavior of the calculated turbulence properties is consistent with exact results and the correct limiting values for these properties are recovered. Compressibility effects are found to have a negative influence on turbulent mixing which is reflected in a reduction of the maximum value of the turbulent kinetic energy and the value of the viscous dissipation at the wall as the free-stream Mach number increases. Wall cooling also produces the same effects and the two versions of the proposed $K-\varepsilon$ model mimic the trend very well. This means that Morkovin's hypothesis is valid for the full range of Mach numbers and wall temperatures tested, provided that the near-wall two-equation models used to close the governing equations are asymptotically correct and internally consistent in the near-wall region. On the other hand, the well accepted $K-\omega$ model provides good correlations with measurements for the mean velocity and wall shear stress only. Its predictions of the temperature profiles are in considerable error, particularly for high free-stream Mach numbers and for the cooled-wall boundary condition. The reason for these discrepancies is traced to the model's inability to reproduce the near-wall turbulence properly; the modeled asymptotic behavior of the turbulence properties is not consistent with the exact equations governing the transport of these quantities. Despite these deficiencies, it is still rather surprising how well the $K-\omega$ model predicts the mean velocity and skin friction at high Mach numbers.

Considering the excellent results obtained in this paper for equilibrium turbulent boundary layers, future applications of this compressible $K-\varepsilon$ model are planned for the study of more complex non-equilibrium boundary-layer flows involving shocks. In these applications, we would expect the explicit compressible terms appearing in the modeled transport equations for K and ε_s to play a more important role. After these further tests are completed, we will have a much better idea of the full range of applicability of this new compressible $K-\varepsilon$ model for wall-bounded turbulent flows.

ACKNOWLEDGEMENT

Funding support for the first and second authors under Grant No. NAG-1-1080 from NASA Langley Research Center, Hampton, Virginia 23665, is gratefully acknowledged. The grant is monitored by Dr. T. B. Gatski.

REFERENCES

[1]Patel, V. C., Rodi, W., and Scheuerer, G., "Turbulence Models for Near-Wall and Low Reynolds Number Flows: A Review," *AIAA J.*, Vol. 23, 1985, pp. 1308-1319.

[2]Myong, H. K. and Kasagi, N., "A New Approach to the Improvement of $K-\varepsilon$ Turbulence Model for Wall-Bounded Shear Flows," *JSME International Journal*, Vol. 33, 1990, pp. 63-72.

[3]Speziale, C. G., Abid, R., and Anderson, E. C., "A Critical Evaluation of Two-Equation Models for Near-Wall Turbulence," *AIAA Paper 90-1481*, 1990.

[4]Morkovin, M., "Effects of Compressibility on Turbulent Flows," *Mecanique de la Turbulence, CNRS*, (A. Favre ed.) pp. 367-380, Gordon & Breach, 1964.

[5]Bradshaw, P., Launder, B. E., and Lumley, J. L., "Collaborative Testing of Turbulence Models," *ASME J. Fluids Engineering*, Vol. 113, 1991, pp. 3-4.

[6]Huang, P. G., Bradshaw, P., and Coakley, T. J., "Assessment of Closure Coefficients for Compressible - Flow Turbulence Models," *AIAA J.*, submitted for publication.

[7]Bushnell, D. M., "Turbulence Modeling in Aerodynamic Shear Flows," *AIAA Paper No. 91-0214*, 1991.

[8]So, R. M. C., Zhang, H. S., and Speziale, C. G., "Near-Wall Modeling of the Dissipation Rate Equation," *AIAA J.*, in press.

[9]Sarkar, S., Erlebacher, G., Hussaini, M. Y., and Kreiss, H. O., "The Analysis and Modeling of Dilatational Terms in Compressible Turbulence," *J. Fluid Mech.*, Vol. 227, 1991, pp. 473-493.

[10]Sarkar, S., "Modeling the Pressure-Dilatation Correlation," ICASE Report No. 91-42, 1991, NASA Langley Research Center.

[11]Coleman, G. N. and Mansour, N. N., "Simulation and Modeling of Homogeneous Compressible Turbulence under Isotropic Mean Compression," *Eighth Symposium on Turbulent Shear Flows*, 1991, Munich, Germany.

[12]Wilcox, D. C., "Reassessment of the Scale-Determining Equation for Advanced Turbulence Models," *AIAA J.*, Vol. 26, 1988, pp. 1299-1310.

[13]Speziale, C. G. and Sarkar, S., "Second-Order Closure Models for Supersonic Turbulent Flows," *AIAA Paper 91-0217*, 1991.

[14]Rodi, W., "A New Algebraic Relation for Calculating Reynolds Stresses," *ZAMM*, Vol. 56, 1976, pp. T219-221.

[15]Speziale, C. G., "On Nonlinear $K-\ell$ and $K-\varepsilon$ Models of Turbulence," *J. Fluid Mech.*, Vol. 178, 1987, pp. 459-475.

[16]Schlichting, H., *Boundary Layer Theory*, McGraw-Hill, New York, 1975.

[17]So, R. M. C., Lai, Y. G., Zhang, H. S., and Hwang, B. C., "Near-Wall Second-Order Turbulence Closures: A Review," *AIAA J.*, 1991, to appear; also NASA CR-4369, 1991.

[18]Zhang, H. S. and So, R. M. C., "Asymptotically Correct Near-Wall Models for Boundary-Layer Flows," *Proceedings of the Fourth International Symposium on Computational Fluid Dynamics*, 1991, pp. 1348-1353.

[19]Sommer, T. P., So, R. M. C., and Lai, Y. G., "Near-Wall Closures for Non-Buoyant Flows with Heat Transfer," *Proceedings of the Fourth International Symposium on Computational Fluid Dynamics*, 1991, pp. 1077-1082.

[20]Kim, J., Moin, P., and Moser, R. D., "Turbulence Statistics in Fully Developed Channel Flow at Low Reynolds Number," *J. Fluid Mech.*, Vol. 177, 1987, pp. 133-186.

[21]Mansour, N. N., Kim, J., and Moin, P., "Reynolds-Stress and Dissipation-Rate Budgets in a Turbulent Channel Flow," *J. Fluid Mech.*, Vol. 194, 1988, pp. 15-44.

[22]Spalart, P. R., "Direct Simulation of a Turbulent Boundary Layer up to $R_\theta = 1410$," *J. Fluid Mech.*, Vol. 187, 1988, pp. 61-98.

[23]Kim, J. and Moin, P., "Transport of Passive Scalars in a Turbulent Channel Flow," *Turbulent Shear Flows 6*, Springer-Verlag, Berlin, 1989, pp. 85-96.

[24]Kasagi, N., Tomita, Y., and Kuroda, A., "Direct Numerical Simulation of the Passive Scalar Field in a Two-Dimensional Turbulent Channel Flow," *3rd ASME-JSME Thermal Engineering Joint Conference*, Reno, March, 1991.

[25]Klebanoff, P. S., "Characteristics of Turbulence in a Boundary Layer with Zero Pressure Gradient," *NACA TN-1247*, 1955.

[26]Cebeci, T. and Smith, A. M. O., *Analysis of Turbulent Boundary Layers*, Academic Press, New York, 1974.

[27]Anderson, E. C. and Lewis, C. H., "Laminar or Turbulent Boundary-Layer Flows of Perfect Gases or Reacting Gas Mixtures in Chemical Equilibrium," NASA CR-1893, 1971.

[28]Fernholz, H. H. and Finley, P. J., "A Critical Compilation of Compressible Turbulent Boundary Layer Data," *AGARDograph No. 223*, 1977.

[29]Kline, S. J., Cantwell, B. J., and Lilley, G. M. (eds.), *Proceedings of the 1980-81 AFOSR-HTTM-Stanford Conference on Complex Turbulent Flows*, Stanford University Press, Stanford, CA, 1981.

[30]van Driest, E. R., "Turbulent Boundary Layer in Compressible Fluids," *Journal of Aeronautical Sciences*, Vol. 18, 1951, pp. 145-160 and 216.

[31]Maise, G. and McDonald, H., "Mixing Length and Kinematic Eddy Viscosity in a Compressible Boundary Layer," *AIAA J.*, Vol. 6, 1968, pp. 73-80.

[32]Lai, Y. G. and So, R. M. C., "Near-Wall Modeling of Turbulent Heat Fluxes," *International Journal of Heat and Mass Transfer*, Vol. 33, 1990, pp. 1429-1440.

Case	M_∞	T_w/T_r	Model	a_k	$a_{uv} \times 10^4$	$k^+/\varepsilon_s^+(y_w^+)^2$
55010504	2.244	1.0	$K-\varepsilon$ model/1	0.0998	7.167	0.50
55010504	2.244	1.0	$K-\varepsilon$ model/2	0.0992	7.198	0.50
53011302	4.544	1.0	$K-\varepsilon$ model/1	0.0850	6.700	0.50
53011302	4.544	1.0	$K-\varepsilon$ model/2	0.0836	6.760	0.50
73050504	10.31	1.0	$K-\varepsilon$ model/1	0.0785	6.630	0.50
73050504	10.31	1.0	$K-\varepsilon$ model/2	0.0771	6.740	0.50
59020105	5.29	0.92	$K-\varepsilon$ model/1	0.0805	6.120	0.50
59020105	5.29	0.92	$K-\varepsilon$ model/2	0.0788	6.140	0.50

Table 1. Asymptotic near-wall behavior of the calculated turbulence properties.

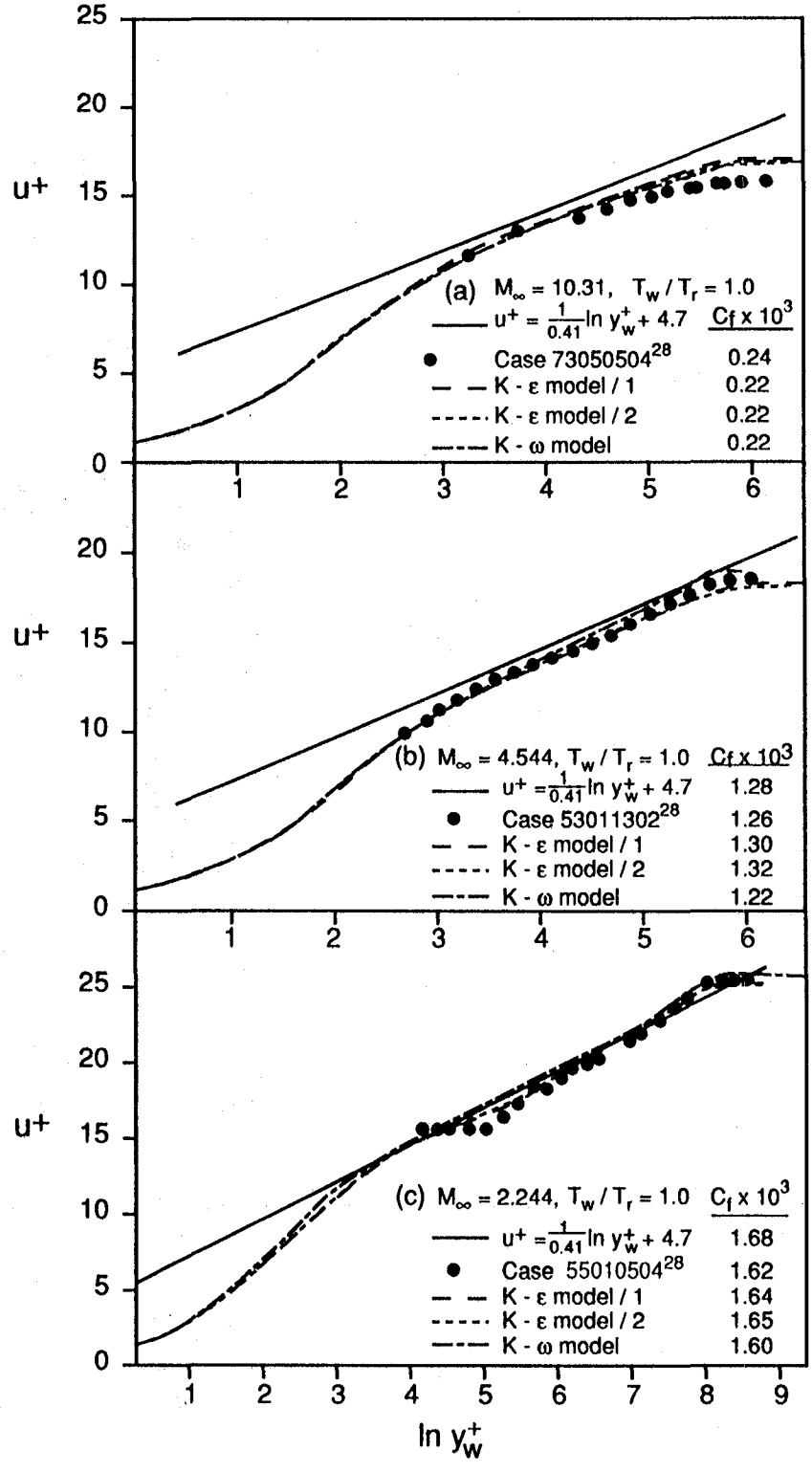

Figure 1. Semi-log plots of u^+ for adiabatic wall boundary condition: (a) $M_\infty = 10.31$, (b) $M_\infty = 4.544$, and (c) $M_\infty = 2.244$.

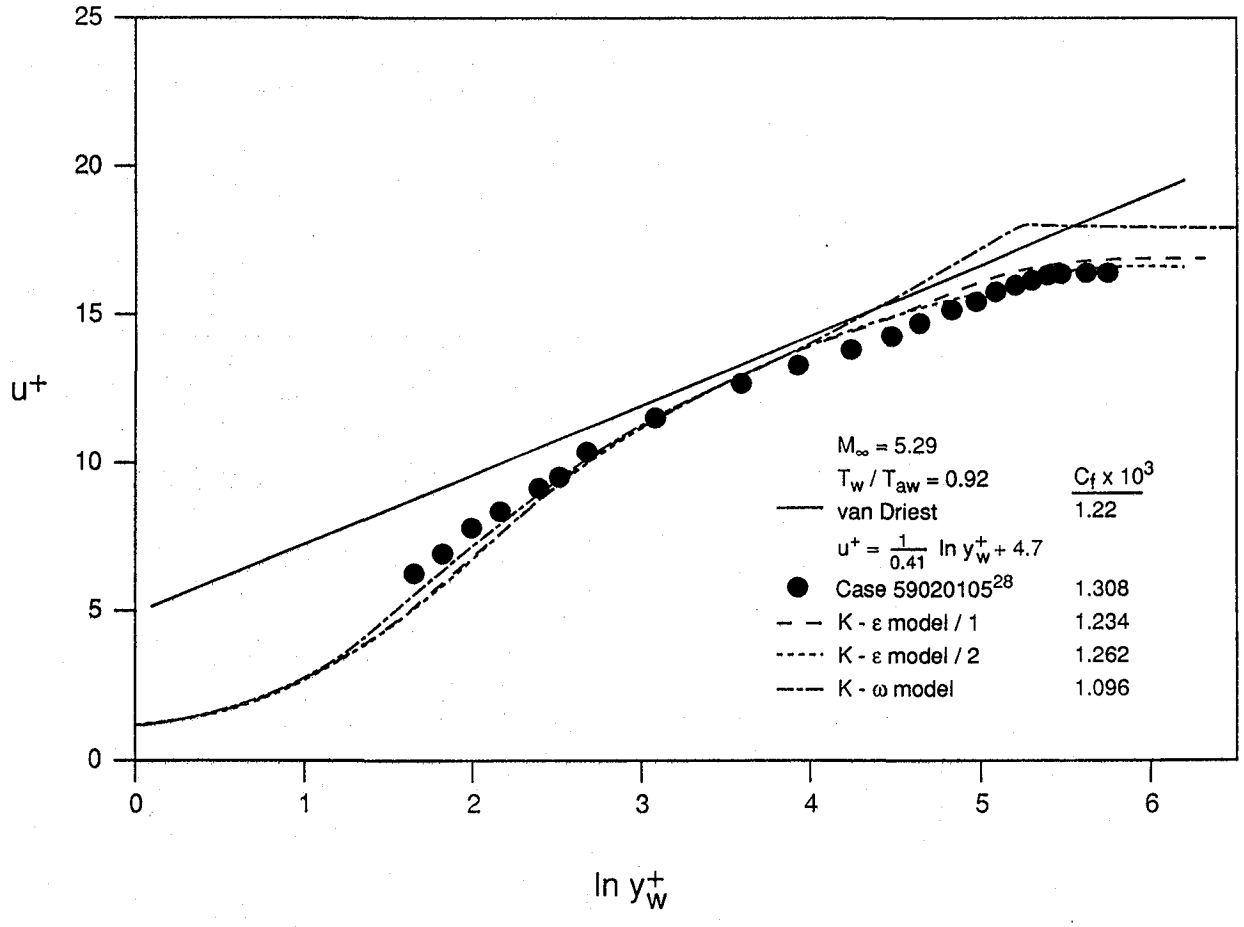

Figure 2. Semi-log plots of u^+ for cooled wall boundary condition.

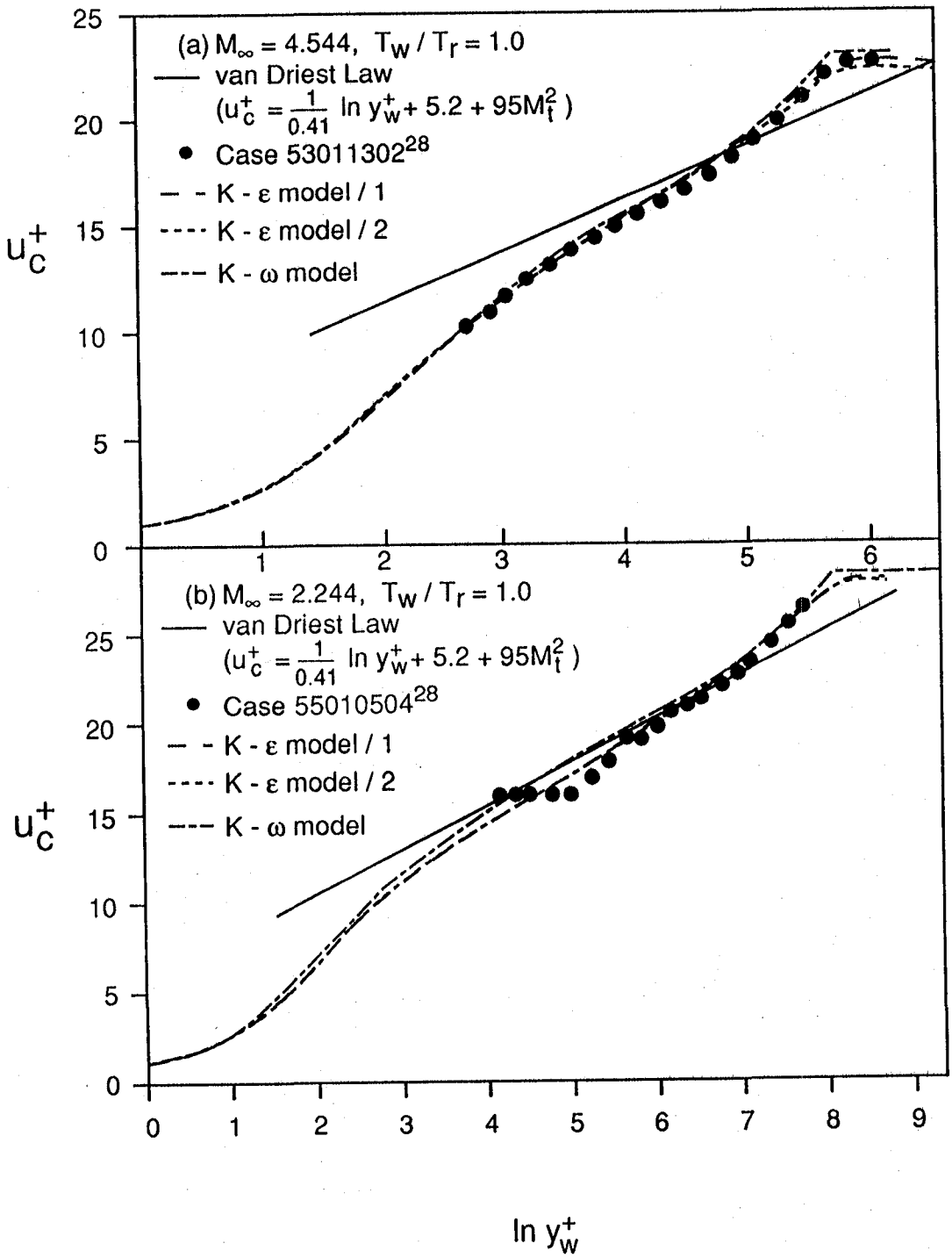

Figure 3. Semi-log plots of u_c^+ for two different M_∞: (a) $M_\infty = 4.544$ and (b) $M_\infty = 2.244$.

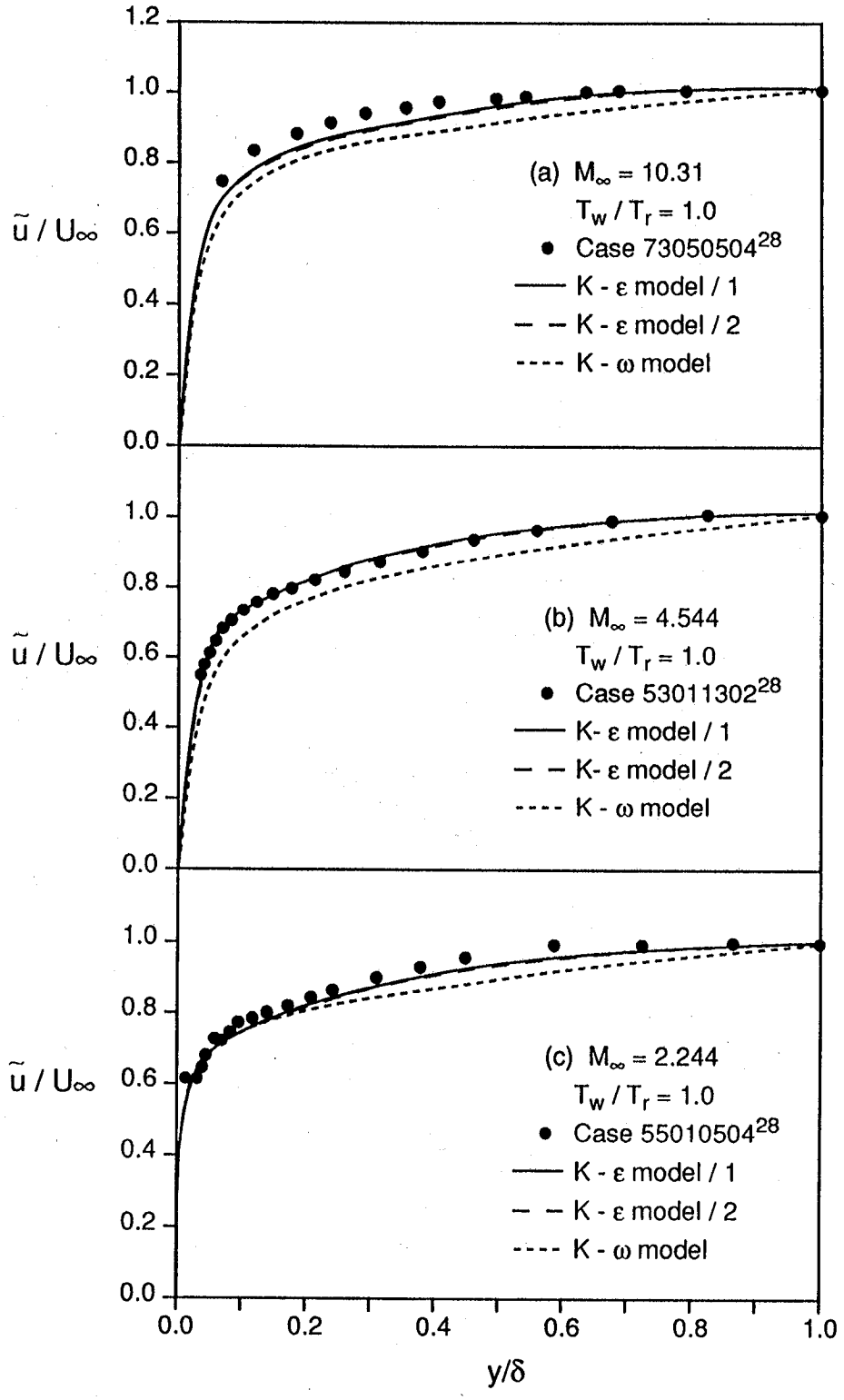

Figure 4. Linear plots of $\tilde{u}/U_\infty$ for adiabatic wall boundary condition: (a) $M_\infty = 10.31$, (b) $M_\infty = 4.544$, and (c) $M_\infty = 2.244$.

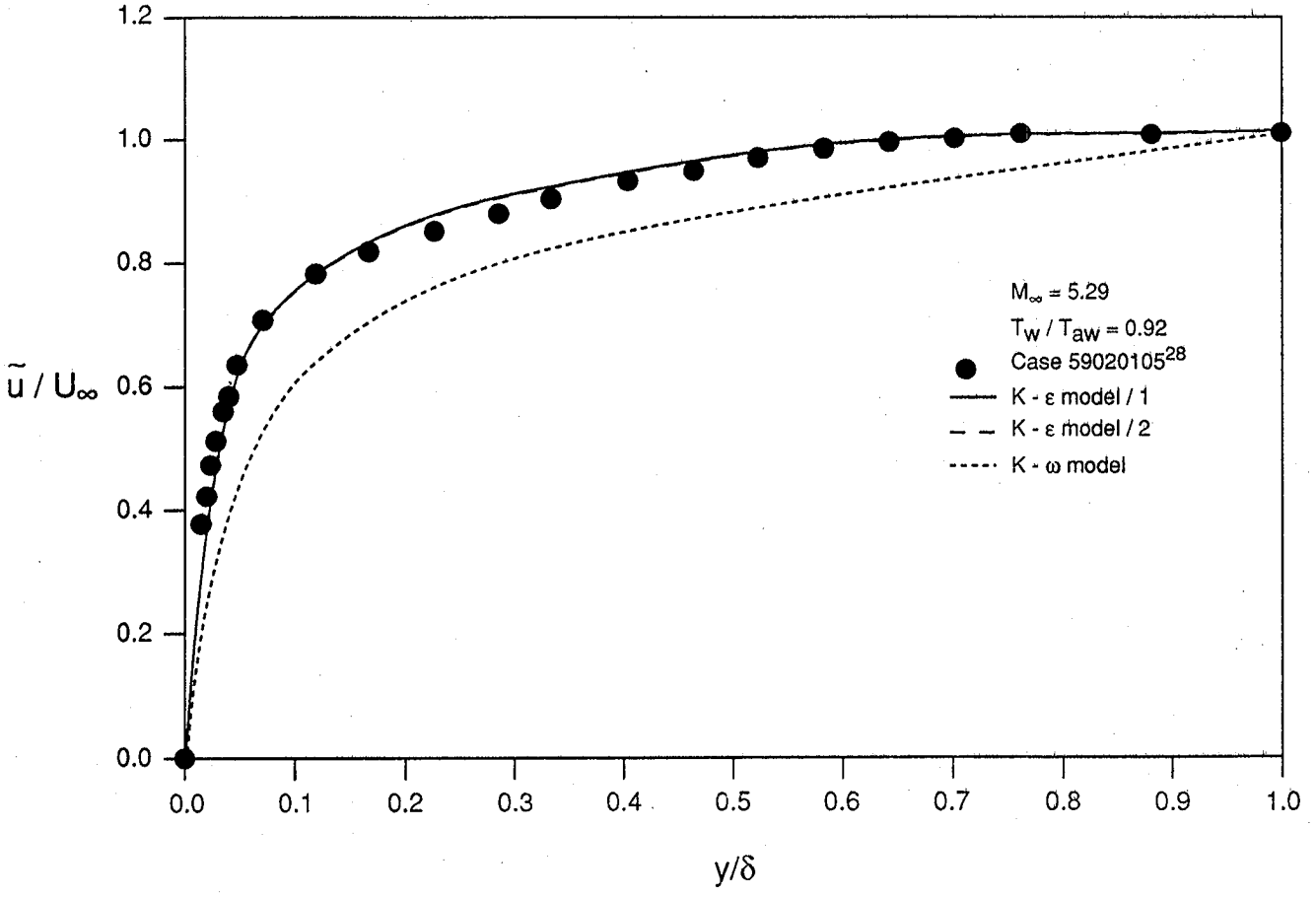

Figure 5. Linear plots of $\tilde{u}/U_\infty$ for cooled wall boundary condition.

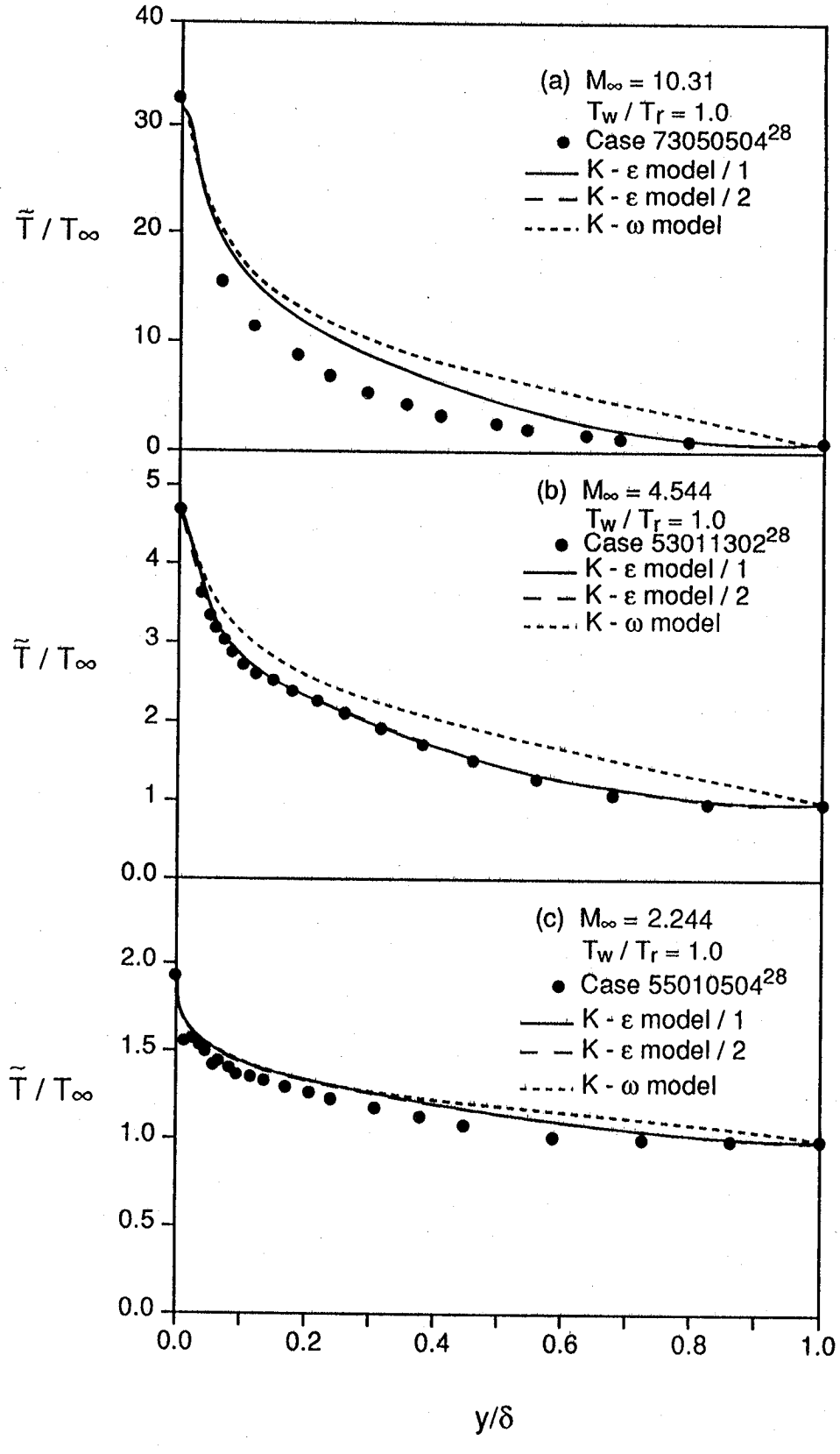

Figure 6. Linear plots of $\tilde{T}/T_\infty$ for adiabatic wall boundary condition: (a) $M_\infty = 10.31$, (b) $M_\infty = 4.544$, and (c) $M_\infty = 2.244$.

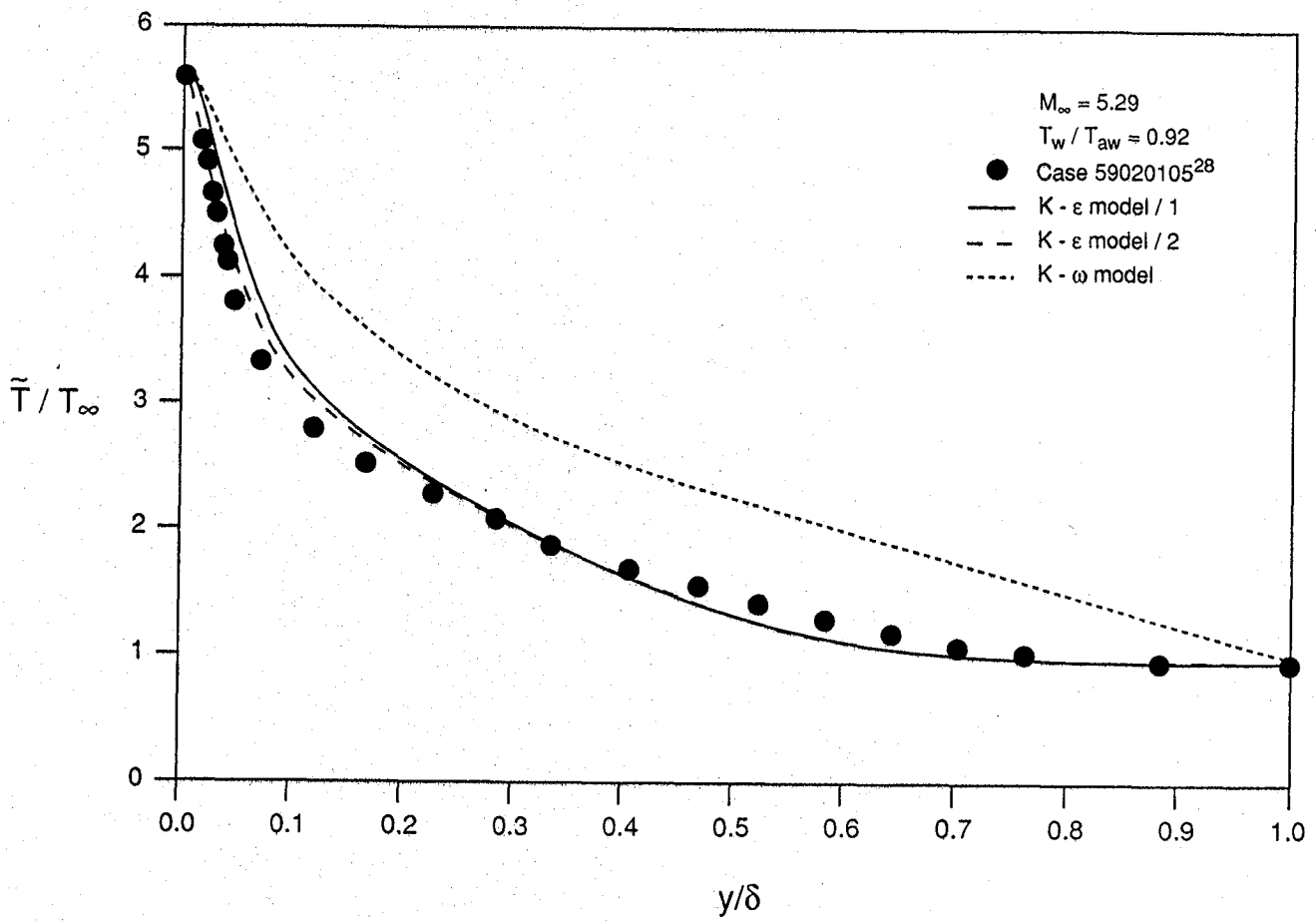

Figure 7. Linear plots of $\tilde{T}/T_\infty$ for cooled wall boundary condition.

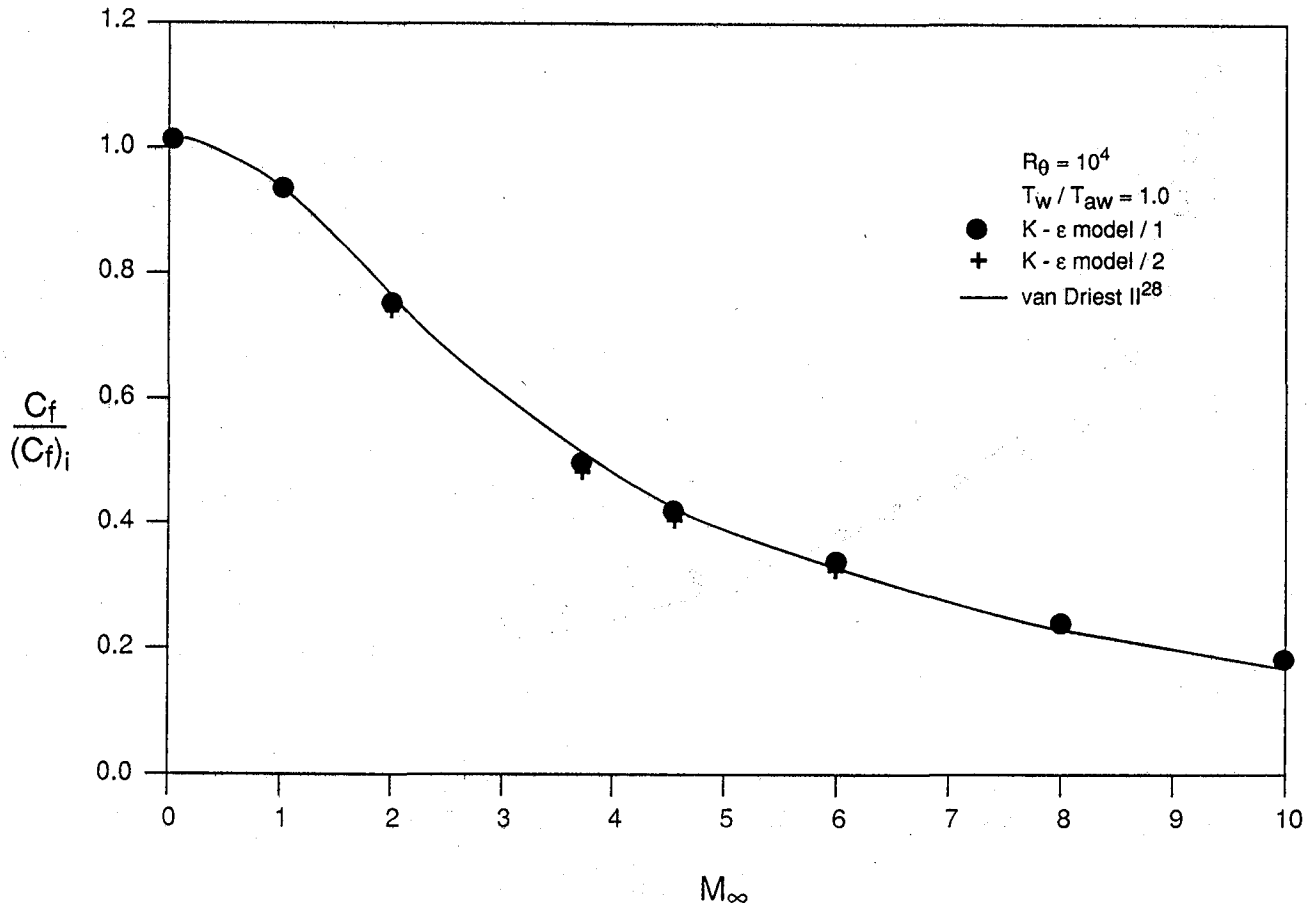

Figure 8. Variation of $C_f/(C_f)_i$ with M_∞ for adiabatic wall boundary condition.

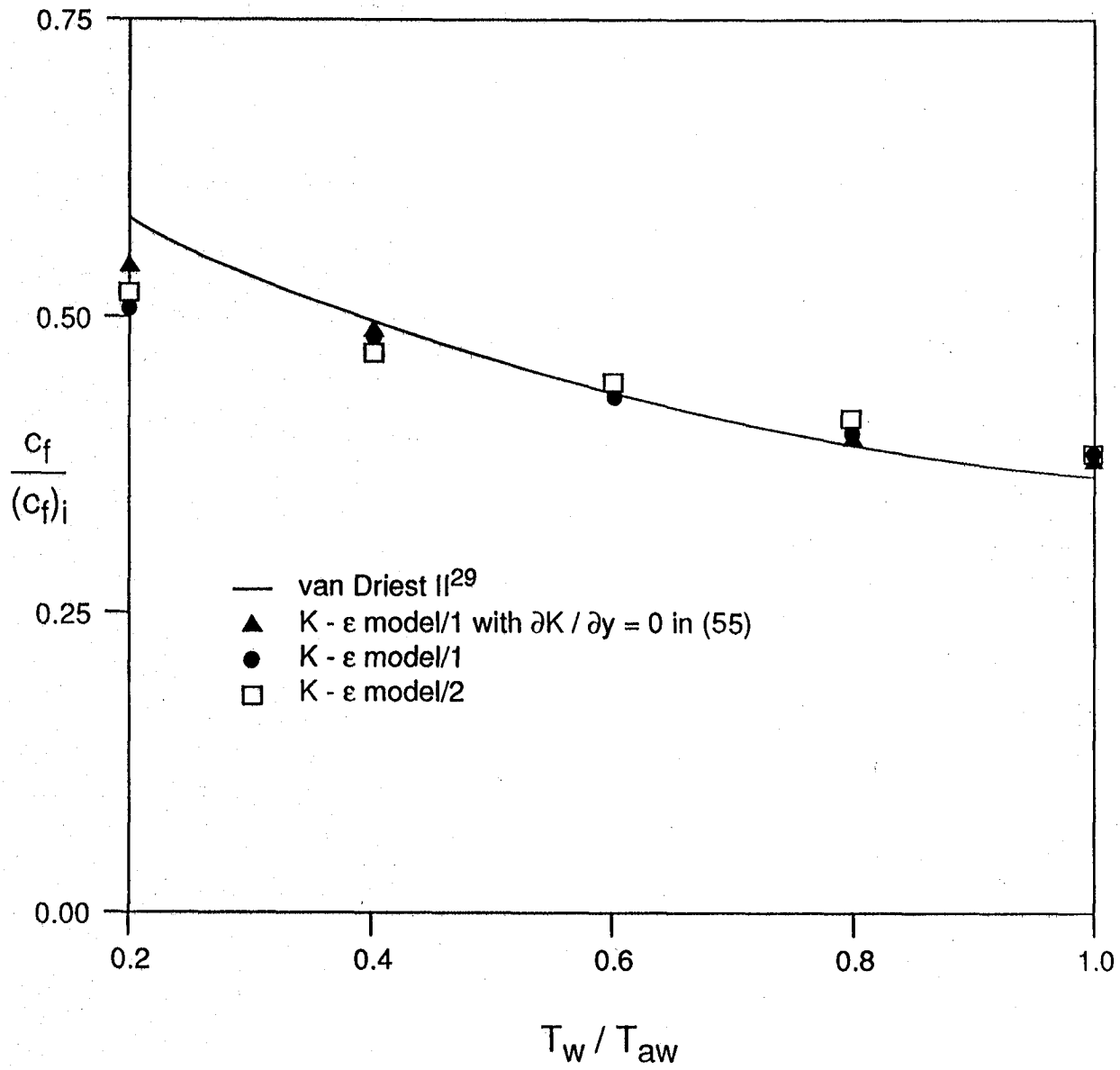

Figure 9. Variation of $C_f/(C_f)_i$ with T_w/T_{aw} for $M_\infty = 5.0$.

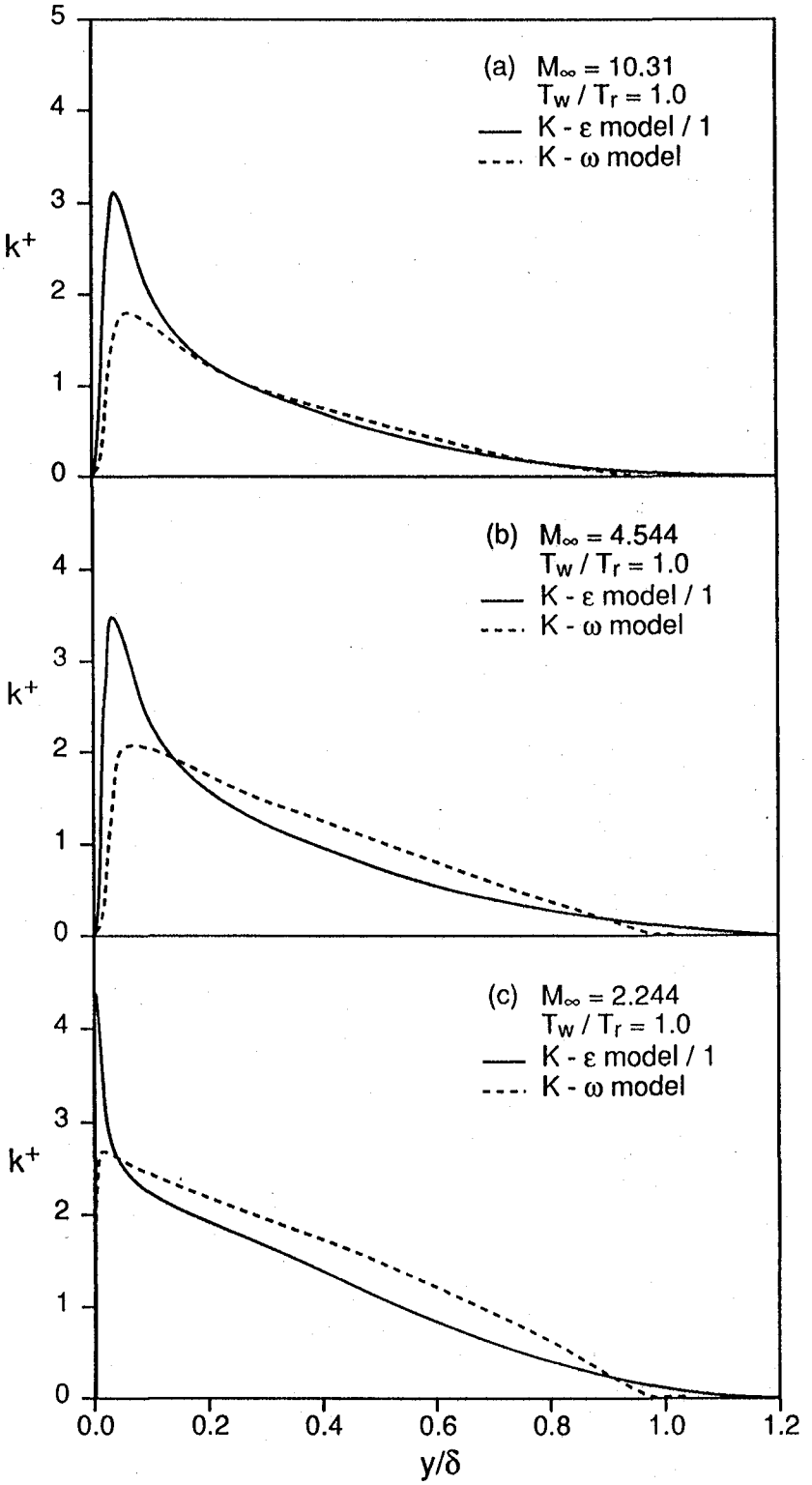

Figure 10. Behavior of k^+ across the boundary layer for adiabatic wall boundary condition: (a) $M_\infty = 10.31$, (b) $M_\infty = 4.544$, and (c) $M_\infty = 2.244$.

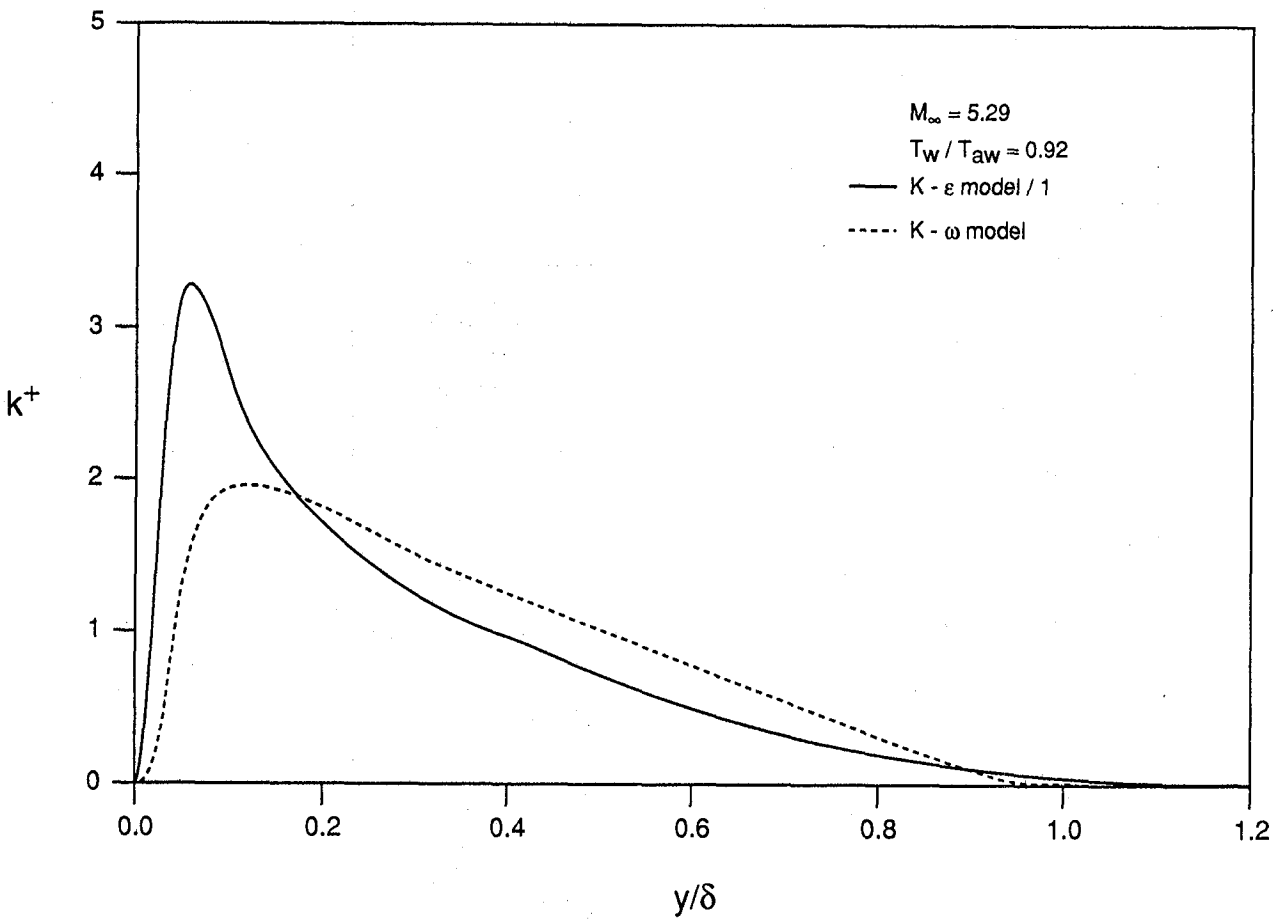

Figure 11. Behavior of k^+ across the boundary layer for cooled wall boundary condition.

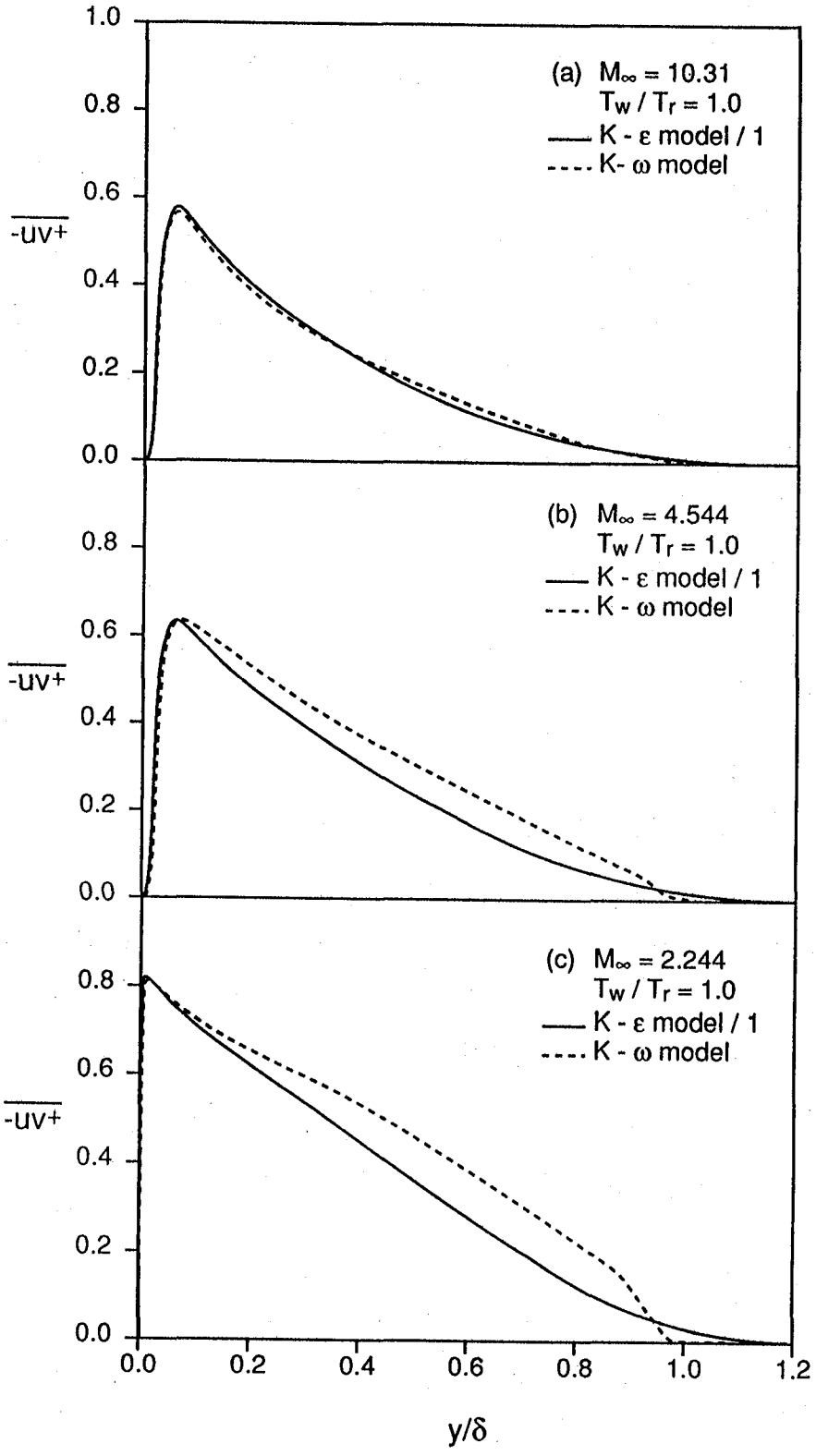

Figure 12. Behavior of $-\overline{uv}^+$ across the boundary layer for adiabatic wall boundary condition: (a) $M_\infty = 10.31$, (b) $M_\infty = 4.544$, and (c) $M_\infty = 2.244$.

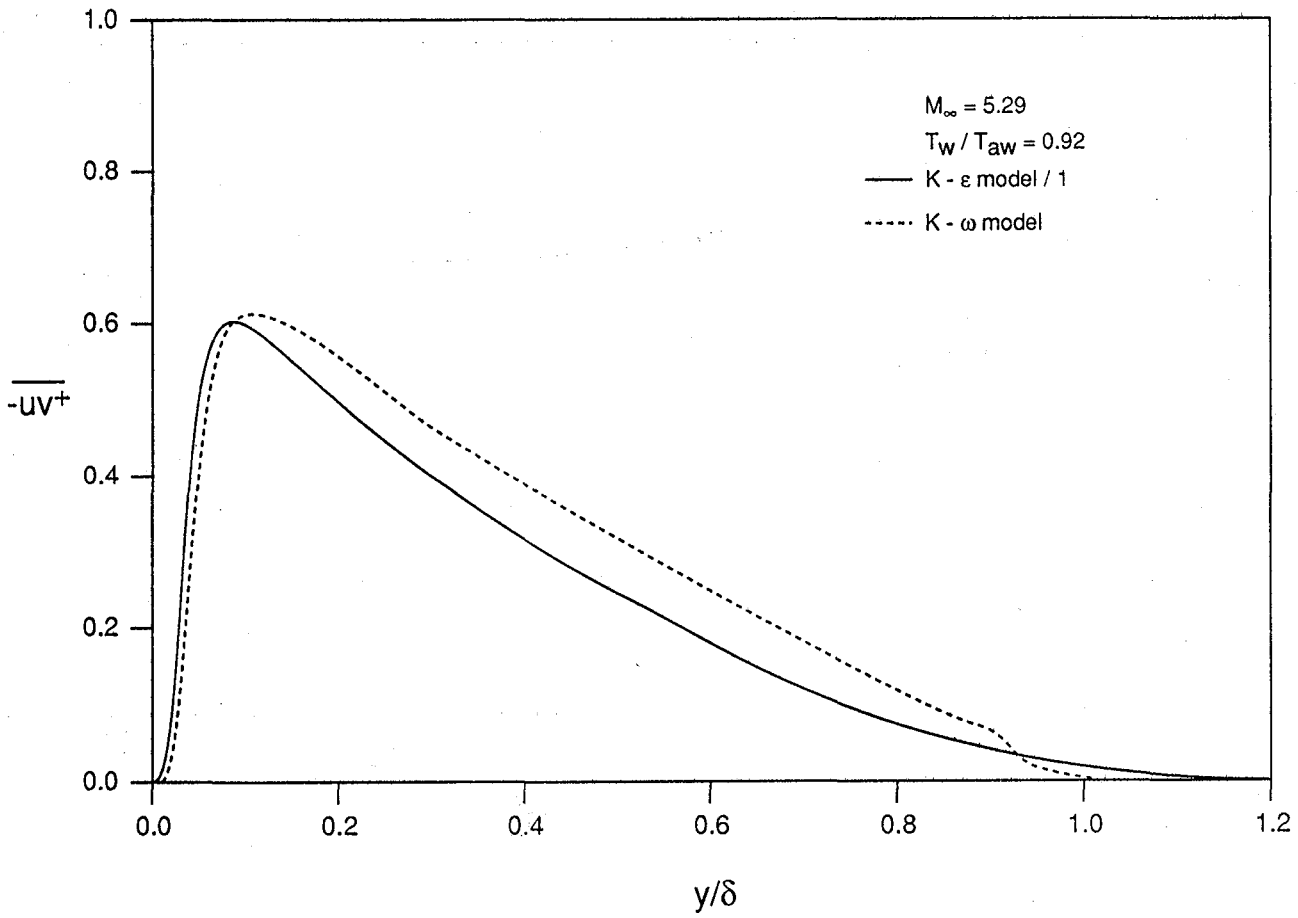

Figure 13. Behavior of $-\overline{uv}^+$ across the boundary layer for cooled wall boundary condition.

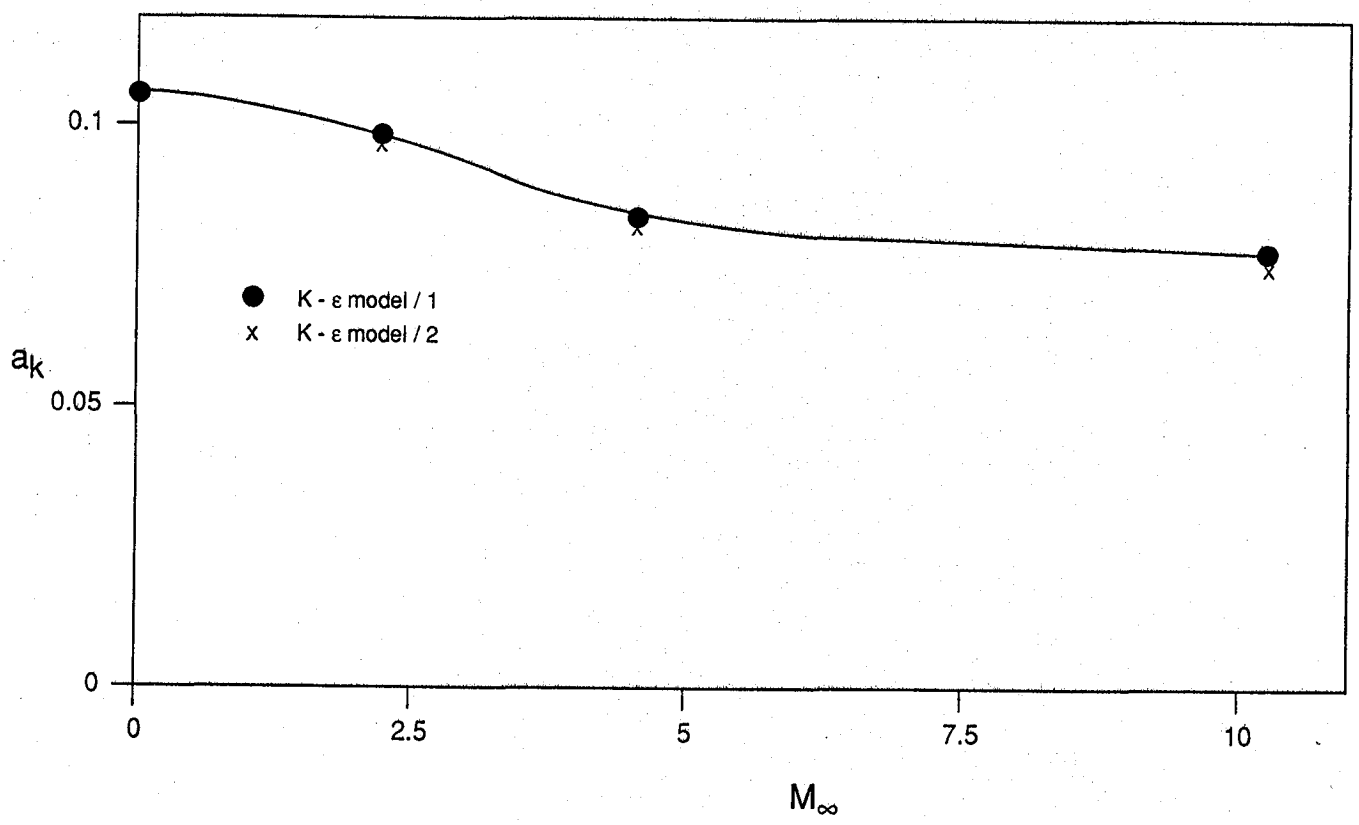

Figure 14. Variation of a_k with M_∞ for adiabatic wall boundary condition.

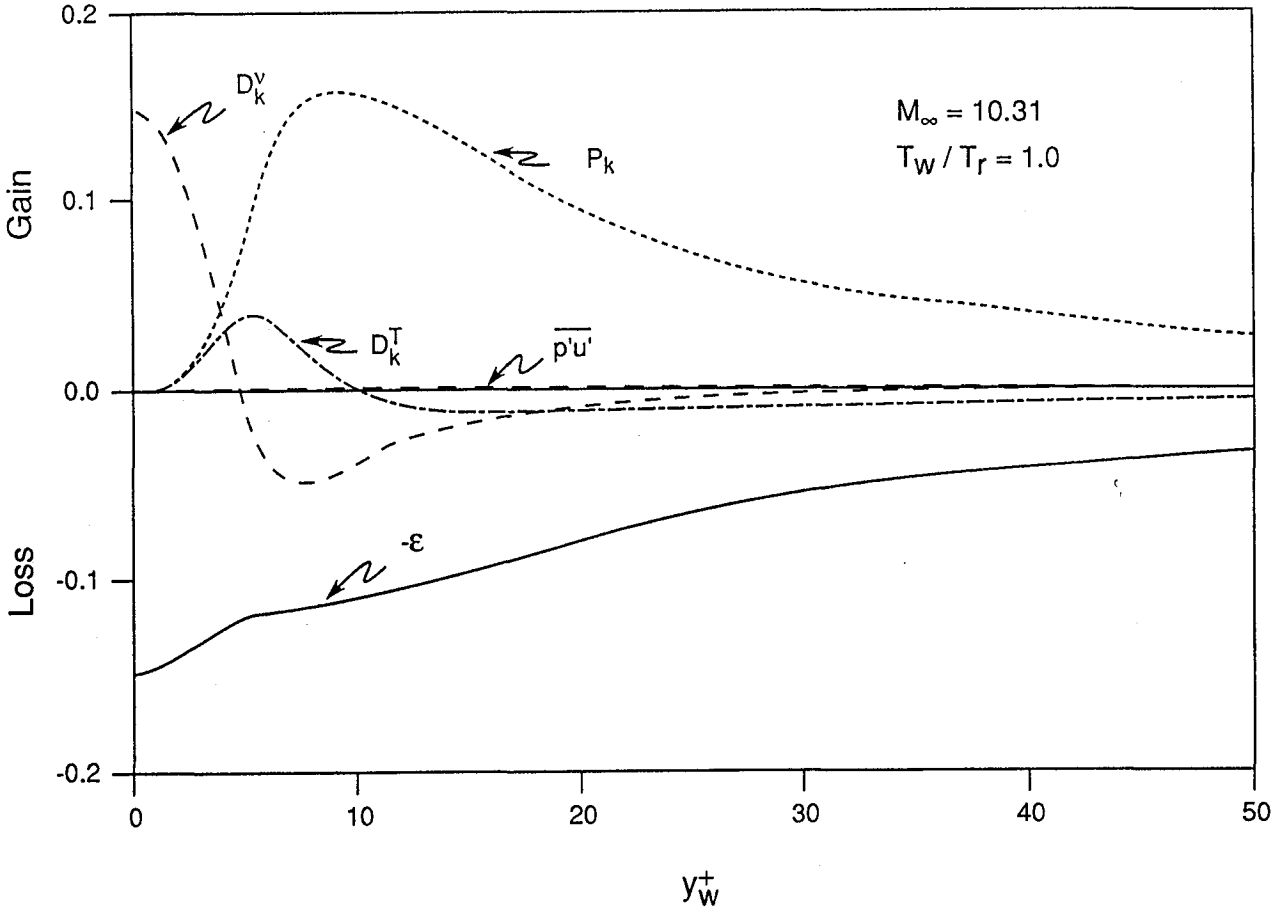

Figure 15. Near-wall budget of K for adiabatic wall boundary condition and $M_\infty = 10.31$.

REPORT DOCUMENTATION PAGE

Form Approved
OMB No. 0704-0188

1. AGENCY USE ONLY (Leave blank)	2. REPORT DATE	3. REPORT TYPE AND DATES COVERED
	November 1991	Contractor Report

4. TITLE AND SUBTITLE
A Near-Wall Two-Equation Model for Compressible Turbulent Flows

5. FUNDING NUMBERS
NAS1-18605
505-90-52-01

6. AUTHOR(S)
H. S. Zhang, R. M. C. So, C. G. Speziale and Y. G. Lai

7. PERFORMING ORGANIZATION NAME(S) AND ADDRESS(ES)
Institute for Computer Applications in Science and Engineering
Mail Stop 132C, NASA Langley Research Center
Hampton, VA 23665-5225

8. PERFORMING ORGANIZATION REPORT NUMBER
ICASE Report No. 91-82

9. SPONSORING/MONITORING AGENCY NAME(S) AND ADDRESS(ES)
National Aeronautics and Space Administration
Langley Research Center
Hampton, VA 23665-5225

10. SPONSORING/MONITORING AGENCY REPORT NUMBER
NASA CR-189565
ICASE Report No. 91-82

11. SUPPLEMENTARY NOTES
Langley Technical Monitor: Michael F. Card
Final Report
To be submitted to AIAA Journal

12a. DISTRIBUTION/AVAILABILITY STATEMENT
Unclassified - Unlimited

Subject Category 34

12b. DISTRIBUTION CODE

13. ABSTRACT *(Maximum 200 words)*

A near-wall two-equation turbulence model of the K-ε type is developed for the description of high-speed compressible flows. The Favre-averaged equations of motion are solved in conjunction with modeled transport equations for the turbulent kinetic energy and solenoidal dissipation wherein a variable density extension of the asymptotically consistent near-wall model of So and co-workers is supplemented with new dilatational models. The resulting compressible two-equation model is tested in the supersonic flat plate boundary layer -- with an adiabatic wall and with wall cooling -- for Mach numbers as large as 10. Direct comparisons of the predictions of the new model with raw experimental data and with results from the K-ω model indicate that it performs well for a wide range of Mach numbers. The surprising finding is that the Morkovin hypothesis, where turbulent dilatational terms are neglected, works well at high Mach numbers provided that the near wall model is asymptotically consistent. Instances where the model predictions deviate from the experiments appear to be attributable to the assumption of constant turbulent Prandtl number -- a deficiency that will be addressed in a future paper.

14. SUBJECT TERMS	15. NUMBER OF PAGES
compressible turbulence modeling; near-wall two-equation models; supersonic boundary layers	37
	16. PRICE CODE A03

17. SECURITY CLASSIFICATION OF REPORT	18. SECURITY CLASSIFICATION OF THIS PAGE	19. SECURITY CLASSIFICATION OF ABSTRACT	20. LIMITATION OF ABSTRACT
Unclassified	Unclassified		

NSN 7540-01-280-5500

Standard Form 298 (Rev. 2-89)
Prescribed by ANSI Std. Z39-18
298-102

NASA-Langley, 1991